

Narrowest Significance Pursuit: inference for multiple change-points in linear models

Piotr Fryzlewicz*

October 20, 2022

Abstract

We propose Narrowest Significance Pursuit (NSP), a general and flexible methodology for automatically detecting localised regions in data sequences which each must contain a change-point (understood as an abrupt change in the parameters of an underlying linear model), at a prescribed global significance level. NSP works with a wide range of distributional assumptions on the errors, and guarantees important stochastic bounds which directly yield exact desired coverage probabilities, regardless of the form or number of the regressors. In contrast to the widely studied “post-selection inference” approach, NSP paves the way for the concept of “post-inference selection”. An implementation is available in the R package `nsp`.

Keywords: confidence intervals, structural breaks, post-selection inference, wild binary segmentation, narrowest-over-threshold.

*Department of Statistics, London School of Economics, Houghton Street, London WC2A 2AE, UK.
Email: p.fryzlewicz@lse.ac.uk.

1 Introduction

Examining or monitoring data sequences for abrupt changes (change-points) in their behaviour is an important task in a variety of fields. Having to discriminate between significant (real) changes and random fluctuations points to the importance of statistical inference in multiple change-point problems. In this paper, we propose a new generic methodology for determining, for a given data sequence and at a given global significance level, localised regions of the data that each must contain a change-point. We define a change-point in Y_t on an interval $[s, e]$ as a departure, on that interval, from a linear model for Y_t with respect to pre-specified regressors. We now give examples of scenarios covered by the proposed methodology.

Scenario 1. *Piecewise-constant signal plus noise model.*

$$Y_t = f_t + Z_t, \quad t = 1, \dots, T, \quad (1)$$

where f_t is a piecewise-constant vector with an unknown number N and locations $0 = \eta_0 < \eta_1 < \dots < \eta_N < \eta_{N+1} = T$ of change-points, and Z_t is zero-centred noise; we give examples of permitted joint distributions of Z_t below. The location η_j is a change-point if $f_{\eta_j-1} = f_{\eta_j}$ but $f_{\eta_j} \neq f_{\eta_j+1}$.

Scenario 2. *Piecewise-polynomial (e.g. piecewise-constant or piecewise-linear) signal plus noise model.* In (1), f_t is a piecewise-polynomial vector, in which the polynomial pieces have a fixed degree $q \geq 0$, assumed known to the analyst. The location η_j is a change-point if f_t can be described as a polynomial vector of degree q on $[\eta_j - q - 1, \eta_j]$, but not on $[\eta_j - q, \eta_j + 1]$.

Scenario 3. *Linear regression with piecewise-constant parameters.* For a given design matrix $X = (X_{t,i})$, $t = 1, \dots, T$, $i = 1, \dots, p$, the response Y_t follows the model

$$Y_t = X_{t,\cdot} \beta^{(j)} + Z_t \quad \text{for } t = \eta_j + 1, \dots, \eta_{j+1}, \quad j = 0, \dots, N, \quad (2)$$

where the parameter vectors $\beta^{(j)} = (\beta_1^{(j)}, \dots, \beta_p^{(j)})'$ are such that $\beta^{(j)} \neq \beta^{(j+1)}$.

Each of these scenarios is a generalisation of the preceding one: Scenario 3 reduces to Scenario 2 if $p = q + 1$ and the i th column of X is a polynomial in t of degree $i - 1$. We permit a broad range of distributional assumptions for Z_t ; we cover i.i.d. Gaussianity and other light-tailed distributions, and we use self-normalisation to also handle (not necessarily known) distributions within the Gaussian domain of attraction, including under heterogeneity. In addition, in Section 3, we introduce Scenario 4, a generalisation of Scenario 3, which provides a framework for the use of our methodology under regression with autoregression (AR). Finally, Section I.1 of the appendix addresses the case in which Z_t 's are autocorrelated. We now review the existing literature on uncertainty in multiple change-point problems which seeks to make confidence statements about the existence or locations of change-points in particular regions of the data, or significance statements about their importance.

In the i.i.d. Gaussian piecewise-constant model, SMUCE (Frick et al., 2014) estimates the number N of change-points as the minimum among those candidate fits \hat{f}_t for which the empirical residuals pass a certain test at level α . An issue for SMUCE, discussed e.g. in Chen et al. (2014), is that the smaller the significance level α , the more lenient the test on the empirical residuals, and therefore the higher the risk of underestimating N . This leads to the counter-intuitive behaviour of the coverage properties of SMUCE illustrated in Chen et al. (2014). SMUCE₂ (Chen et al., 2014) remedies this issue, but still requires that the number of estimated change-points agrees with the truth for successful coverage. As the accurate estimation of N is a well-known difficult problem in low signal-to-noise scenarios, SMUCE₂ is also at risk of being unable to cover the truth with a high nominal probability requested by the user. In the approach taken in this paper, this issue does not arise as we shift the inferential focus away from N . SMUCE is extended to heterogeneous Gaussian noise in Pein et al. (2017) and to dependent data in Dette et al. (2020).

Some authors approach uncertainty quantification for multiple change-point problems from the point of view of post-selection inference (PSI, a.k.a. selective inference); these include Hyun et al. (2018), Hyun et al. (2021), Jewell et al. (2022) and Duy et al. (2020). To ensure

valid inference, PSI conditions on many aspects of the estimation process, which tends to produce p -values with somewhat complex definitions. PSI also does not permit the selection of the tuning parameters of the inference procedure (e.g. the bandwidth h in Jewell et al. (2022)) from the same data. Notwithstanding their usefulness in assessing the significance of previously estimated change-points, these PSI approaches share the following features: (a) they do not consider uncertainties in estimating change-point locations, (b) they do not provide regions of globally significant change in the data, (c) they define significance for each change-point separately, as opposed to globally, (d) they rely on a particular base change-point detection method with its potential strengths or weaknesses. Our approach explicitly contrasts with these features; in particular, in contrast to post-selection inference, it can be described as enabling “post-inference selection”, as we argue later on.

A number of authors (Yao, 1988; Fryzlewicz, 2014; Baranowski et al., 2019; Wang et al., 2021) provide simple consistency results for the number and locations of detected change-points, but in inferential terms, such results are usually difficult to use in practice, as the probability statements involve unknown and hard-to-estimate constants, and the significance level used usually tends to 0 with T , rather than being a user-fixable constant.

Some authors provide simultaneous asymptotic distributional results for the distance between the estimated change-point locations and the truth. In the linear regression context, this is done in Bai and Perron (1998, 2003), and in the piecewise-constant signal plus noise model – in Eichinger and Kirch (2018). These approaches are asymptotic, conditional on the estimated change-point locations, and involve unknown quantities. In contrast, our methodology has a finite-sample nature, makes no assumptions on the signal, and unconditionally and automatically flags up regions of data that must (at a given global significance level) contain change. A further discussion of the differences between our approach and that of Bai and Perron (1998, 2003) can be found in Section A of the appendix.

Inference for multiple change-points is also sometimes posed as control of the False Discovery Rate (FDR), see e.g. Li and Munk (2016), Hao et al. (2013) and Cheng et al. (2020). However, control of FDR is too weak a criterion when one wants to obtain local regions of globally significant change, as we do in this work; this is because FDR is focused on the

number of change-points rather than on their locations.

Bayesian approaches to uncertainty quantification in multiple change-point problems are considered e.g. in Fearnhead (2006) and Nam et al. (2012) (see also the monograph Ruanaidh and Fitzgerald (1996)), and are particularly useful when clear priors, chosen independently of the data, are available about some features of the signal.

We now summarise our new approach, then situate it in the context of the related literature, and next discuss its novel aspects. The objective of our methodology, called “Narrowest Significance Pursuit” (NSP), is to automatically detect localised regions of the data Y_t , each of which must contain at least one change-point (in a suitable sense determined by the given scenario), at a prescribed global significance level. NSP performs unconditional inference without change-point location estimation, and proceeds as follows. A number M of intervals are drawn from the index domain $[1, \dots, T]$, with start- and end-points chosen either uniformly at random, or over an equispaced deterministic grid. On each interval drawn, Y_t is then checked to see whether or not it locally conforms to the prescribed linear model, with any set of parameters. This check is performed through estimating the parameters of the given linear model locally by minimising a particular multiresolution sup-norm loss, and testing the residuals from this fit via the same norm; self-normalisation is involved if necessary. In the first greedy stage, the shortest interval (if one exists) is chosen on which the test is violated at a certain global significance level α . In the second greedy stage, the selected interval is searched for its shortest sub-interval on which a similar test is violated. This sub-interval is then chosen as the first region of global significance, in the sense that it must (at a global level α) contain a change-point, or otherwise the local test would not have rejected the linear model. The procedure then recursively draws M intervals to the left and to the right of the chosen region (with or without overlap), and stops when no further local regions of global significance can be found.

The following alternative viewpoint on NSP may be helpful. We start with a norm (or more generally this could be a test statistic) with the property that for an interval $[s, e]$, we have $\|y_{s:e}\| = \max_{[s', e'] \subseteq [s, e]} \|y_{s':e'}\|$ for any vector y . We work in a change-point model generally described as $Y_t = f_t + Z_t$ (where, for example, in Scenario 3 we have $f_t = X_{t,\cdot}\beta^{(j)}$ for

$t = \eta_j + 1, \dots, \eta_{j+1}$). Given sets $\mathcal{F}([s, e]) \subseteq \mathbb{R}^{e-s+1}$ for each interval $[s, e]$, we wish to find a set of intervals \mathcal{S} such that with a global probability of at least $1 - \alpha$, for each $[s, e] \in \mathcal{S}$, we have $f_{s:e} \notin \mathcal{S}$. For instance, in Scenario 1, we take each $\mathcal{F}([s, e])$ to be constant vectors. To construct \mathcal{S} , we may in principle take $\mathcal{S} = \{[s, e] : \min_{v \in \mathcal{F}([s, e])} \|Y_{s:e} - v\| > \lambda_\alpha\}$, where $P(\|Z\| > \lambda_\alpha) \leq \alpha$; that this \mathcal{S} has the desired property follows in a straightforward way from its definition. However, the problems with \mathcal{S} defined in this way are that it is computationally infeasible and may contain a large number of overlapping intervals. NSP is an algorithm for extracting a meaningful subset of \mathcal{S} , whose elements are suitably short, i.e. provide localisation of any change-points in f_t . We also explain how λ_α may be determined for different classes of noise distribution, and discuss extensions to settings in which autoregression is present.

Fang et al. (2020), in the piecewise-constant signal plus i.i.d. Gaussian noise model, approximate the tail probability of the maximum CUSUM statistic over all sub-intervals of the data. They then propose an algorithm, in a few variants, for identifying short, non-overlapping segments of the data on which the local CUSUM exceeds the derived tail bound, and hence the segments identified must contain at least a change-point each, at a given significance level. Fang and Siegmund (2020) present results of similar nature for a Gaussian model with lag-one autocorrelation, linear trend, and features that are linear combinations of continuous, piecewise differentiable shapes. The most important high-level differences between NSP and these two approaches are that (a) NSP is ready for use with any user-provided design matrix X , and this requires no new calculations or coding, and yields correct coverage probabilities in finite samples of any length; (b) NSP searches for any deviations from local model linearity with respect to the regressors provided; (c) the results of Fang et al. (2020) and Fang and Siegmund (2020) do not cover our Scenario 3 (linear regression with arbitrary X) or Scenario 2 with linearity but not necessarily continuity, or Scenario 2 with higher-than-linear polynomials; (d) NSP is able to handle regression with autoregression practically in the same way as without, in a stable manner and on arbitrarily short intervals, and does not suffer from having to estimate the unknown (nuisance) AR coefficients accurately. We expand on these points in Section A of the appendix.

We also mention below other main distinctive features of NSP in comparison with the existing literature. NSP is specifically constructed to target the shortest possible significant intervals at every stage of the procedure, and to explore as many intervals as possible while remaining computationally efficient. Moreover, NSP critically relies on what we believe is a new use of the multiresolution sup-norm. On each interval drawn, NSP locally fits the postulated linear model via multiresolution sup-norm minimisation (as opposed to e.g. the more usual OLS or MLE). It then uses the same norm to test the empirical residuals from this fit, which ensures the exactness of the coverage statements furnished by NSP, at a prescribed global significance level, for any finite sample sizes, regardless of the scenario and for any given regressors X . Also, thanks to the fact that multiresolution sup-norms can be interpreted as Hölder-like norms on certain function spaces, NSP naturally extends to the cases of unknown or heterogeneous distributions of Z_t using the functional-analytic self-normalisation framework developed in Račkauskas and Suquet (2001), Račkauskas and Suquet (2003) and related papers. Finally, the use of multiresolution sup-norms means that if simulation needs to be used to determine critical values for NSP, then this can be done in a computationally efficient manner.

Section 2 introduces the NSP methodology and provides the relevant finite-sample coverage theory. Section 3 extends this to NSP under self-normalisation and in the additional presence of autoregression. Section 4 provides finite-sample and traditional large-sample detection consistency and rate optimality results for NSP in Scenarios 1 and 2. Section 5 provides extensive numerical examples under a variety of settings. Section 6 describes two real-data case studies. Complete R code implementing NSP is available in the R package `nsp`. There is an appendix, whose contents are mentioned at appropriate places in the paper. Proofs of our theoretical results are in the appendix.

2 The NSP inference framework

Throughout the section, we use the language of Scenario 3, which includes Scenarios 1 and 2 as special cases. In Scenario 1, the matrix X in (2) is of dimensions $T \times 1$ and has all

entries equal to 1. In Scenario 2, the matrix X is of dimensions $T \times (q + 1)$ and its i th column is given by $(t/T)^{i-1}$, $t = 1, \dots, T$. Scenario 4 (for NSP in the additional presence of autoregression), which generalises Scenario 3, is dealt with in Section 3.2.

2.1 Generic NSP algorithm

We start with a pseudocode definition of the NSP algorithm, in the form of a recursively defined function NSP. In its arguments, $[s, e]$ is the current interval under consideration and at the start of the procedure, we have $[s, e] = [1, T]$; Y (of length T) and X (of dimensions $T \times p$) are as in the model formula (2); M is the (maximum) number of sub-intervals of $[s, e]$ drawn; λ_α is the threshold corresponding to the global significance level α (typical values for α would be 0.05 or 0.1) and τ_L (respectively τ_R) is a functional parameter used to specify the degree of overlap of the left (respectively right) child interval of $[s, e]$ with respect to the region of significance identified within $[s, e]$, if any. The no-overlap case would correspond to $\tau_L = \tau_R \equiv 0$. In each recursive call on a generic interval $[s, e]$, NSP adds to the set \mathcal{S} any globally significant local regions (intervals) of the data identified within $[s, e]$ on which Y is deemed to depart significantly (at global level α) from linearity with respect to X . We provide more details underneath the pseudocode below.

```

1: function NSP( $s, e, Y, X, M, \lambda_\alpha, \tau_L, \tau_R$ )
2:   if  $e - s < 1$  then
3:     RETURN
4:   end if
5:   if  $M \geq \frac{1}{2}(e - s + 1)(e - s)$  then
6:      $M := \frac{1}{2}(e - s + 1)(e - s)$ 
7:     draw all intervals  $[s_m, e_m] \subseteq [s, s + 1, \dots, e]$ ,  $m = 1, \dots, M$ , s.t.  $e_m - s_m \geq 1$ 
8:   else
9:     draw a representative (see description below) sample of intervals  $[s_m, e_m] \subseteq [s, s + 1, \dots, e]$ ,  $m = 1, \dots, M$ , s.t.  $e_m - s_m \geq 1$ 
10:  end if
11:  for  $m \leftarrow 1, \dots, M$  do

```



```

12:       $D_{[s_m, e_m]} := \text{DEVIATIONFROMLINEARITY}(s_m, e_m, Y, X)$ 
13:    end for
14:     $\mathcal{M}_0 := \arg \min_m \{e_m - s_m : m = 1, \dots, M; D_{[s_m, e_m]} > \lambda_\alpha\}$ 
15:    if  $|\mathcal{M}_0| = 0$  then
16:      RETURN
17:    end if
18:     $m_0 := \text{ANYOF}(\arg \max_m \{D_{[s_m, e_m]} : m \in \mathcal{M}_0\})$ 
19:     $[\tilde{s}, \tilde{e}] := \text{SHORTESTSIGNIFICANTSUBINTERVAL}(s_{m_0}, e_{m_0}, Y, X, M, \lambda_\alpha)$ 
20:    add  $[\tilde{s}, \tilde{e}]$  to the set  $\mathcal{S}$  of significant intervals
21:     $\text{NSP}(s, \tilde{s} + \tau_L(\tilde{s}, \tilde{e}, Y, X), Y, X, M, \lambda_\alpha, \tau_L, \tau_R)$ 
22:     $\text{NSP}(\tilde{e} - \tau_R(\tilde{s}, \tilde{e}, Y, X), e, Y, X, M, \lambda_\alpha, \tau_L, \tau_R)$ 
23: end function

```

The NSP algorithm is launched by the pair of calls: $\mathcal{S} := \emptyset$; $\text{NSP}(1, T, Y, X, M, \lambda_\alpha, \tau_L, \tau_R)$. On completion, the output of NSP is in the variable \mathcal{S} . We now comment on the NSP function line by line. In lines 2–4, execution is terminated for intervals that are too short. In lines 5–10, a check is performed to see if M is at least as large as the number of all sub-intervals of $[s, e]$. If so, then M is adjusted accordingly, and all sub-intervals are stored in $\{[s_m, e_m]\}_{m=1}^M$. Otherwise, a sample of M sub-intervals $[s_m, e_m] \subseteq [s, e]$ is drawn in which either (a) s_m and e_m are obtained uniformly and with replacement from $[s, e]$, or (b) s_m and e_m are all possible pairs from an (approximately) equispaced grid on $[s, e]$ which permits at least M such sub-intervals.

In lines 11–13, each sub-interval $[s_m, e_m]$ is checked to see to what extent the response on this sub-interval (denoted by $Y_{s_m:e_m}$) conforms to the linear model (2) with respect to the set of covariates on the same sub-interval (denoted by $X_{s_m:e_m, \cdot}$). For NSP without self-normalisation, described in this section, this check is done by fitting the postulated linear model on $[s_m, e_m]$ using a certain multiresolution sup-norm loss, and computing the same multiresolution sup-norm of the empirical residuals from this fit, to form a measure of deviation from linearity on this interval. This core step of the NSP algorithm is described in more detail in Section 2.2.

In line 14, the measures of deviation obtained in line 12 are tested against threshold λ_α , chosen to guarantee global significance level α . How to choose λ_α depends (only) on the distribution of Z_t ; this question is addressed in Section 2.3 below and in Section D of the appendix. The shortest sub-interval(s) $[s_m, e_m]$ for which the test rejects the local hypothesis of linearity of Y versus X at global level α are collected in set \mathcal{M}_0 . In lines 15–17, if \mathcal{M}_0 is empty, then the procedure decides that it has not found regions of significant deviations from linearity on $[s, e]$, and stops on this interval as a consequence. Otherwise, in line 18, the procedure continues by choosing the sub-interval, from among the shortest significant ones, on which the deviation from linearity has been the largest. (Empirically, \mathcal{M}_0 often has cardinality one, in which case the choice in line 18 is trivial.) The chosen interval is denoted by $[s_{m_0}, e_{m_0}]$.

In line 19, $[s_{m_0}, e_{m_0}]$ is searched for its shortest significant sub-interval, i.e. the shortest sub-interval on which the hypothesis of linearity is rejected locally at a global level α . Such a sub-interval certainly exists, as $[s_{m_0}, e_{m_0}]$ itself has this property. The structure of this search again follows the workflow of the NSP procedure; more specifically, it proceeds by executing lines 2–18 of NSP, but with s_{m_0}, e_{m_0} in place of s, e . The chosen interval is denoted by $[\tilde{s}, \tilde{e}]$. This two-stage search (identification of $[s_{m_0}, e_{m_0}]$ in the first stage and of $[\tilde{s}, \tilde{e}] \subseteq [s_{m_0}, e_{m_0}]$ in the second stage) is crucial in NSP’s pursuit to force the identified intervals of significance to be as short as possible, without unacceptably increasing the computational cost. The importance of this two-stage solution is illustrated in Section E of the appendix. In line 20, the selected interval $[\tilde{s}, \tilde{e}]$ is added to the output set \mathcal{S} .

In lines 21–22, NSP is executed recursively to the left and to the right of the detected interval $[\tilde{s}, \tilde{e}]$. However, we optionally allow for some overlap with $[\tilde{s}, \tilde{e}]$. The overlap, if present, is a function of $[\tilde{s}, \tilde{e}]$ and, if it involves detection of the location of a change-point within $[\tilde{s}, \tilde{e}]$, then it is also a function of Y, X . An example of the relevance of this is given in Section 5.1.1.

In NSP, having $p = p(T)$ growing with T is possible, but we must have $p(T) + 1 \leq T$ or otherwise no regions of significance will be found. Our implementation of NSP is “bottom-up”, in the sense that at each recursive stage, we consider the intervals $[s_m, e_m]$ in non-decreasing

order of their lengths, and exit the current recursive stage (if and) as soon as significance is declared, rather than moving on to longer intervals. This aligns with the objective of looking for the shortest intervals (so the examination of longer intervals is unnecessary if shorter significant intervals have been found). Any non-bottom-up implementation of NSP would therefore unnecessarily be wasting computational resources. This is in contrast to, for example, the region-based multiple testing method of Meijer et al. (2015), in which the successive p -value adjustments (which lead to power improvements) are only possible because of the top-down character of that approach. Section B of the appendix comments on a few other generic aspects of the NSP algorithm.

2.2 Measuring deviation from linearity in NSP

This section completes the definition of NSP (in the version without self-normalisation) by describing the `DEVIATIONFROMLINEARITY` function (NSP algorithm, line 12). Its basic building block is a scaled partial sum statistic, defined for an arbitrary input sequence $\{y_t\}_{t=1}^T$ by $U_{s,e}(y) = (e - s + 1)^{-1/2} \sum_{t=s}^e y_t$. In the literature, scaled partial sum statistics acting directly on the data are often combined into variants of scan statistics (Siegmund and Venkatraman, 1995; Arias-Castro et al., 2005; Jeng et al., 2010; Walther, 2010; Chan and Walther, 2013; Sharpnack and Arias-Castro, 2016; König et al., 2020; Munk et al., 2020). They are also used in estimators represented as the simplest (from the point of view of a certain regularity or smoothness functional) fit to the data for which the empirical residuals are deemed to behave like the true residuals (Frick et al., 2014; Davies and Kovac, 2001; Davies et al., 2009; Li, 2016).

We define the scan statistic of an input vector y (of length T) with respect to the interval set \mathcal{I} as

$$\|y\|_{\mathcal{I}} = \max_{[s,e] \in \mathcal{I}} |U_{s,e}(y)|. \quad (3)$$

The set \mathcal{I} used in NSP contains intervals at a range of scales and locations. For computational efficacy, instead of the set \mathcal{I}^a of all subintervals of $[1, T]$, we use the set \mathcal{I}^d of all intervals of dyadic lengths and arbitrary locations, that is $\mathcal{I}^d = \{[s, e] \subseteq [1, T] : e - s =$

$2^j - 1$, $j = 0, \dots, \lfloor \log_2 T \rfloor$. A simple pyramid algorithm of complexity $O(T \log T)$ is available for the computation of all $U_{s,e}(y)$ for $[s, e] \in \mathcal{I}^d$. We also define restrictions of \mathcal{I}^a and \mathcal{I}^d to arbitrary intervals $[s, e]$ as $\mathcal{I}_{[s,e]}^d = \{[u, v] \subseteq [s, e] : [u, v] \in \mathcal{I}^d\}$, and analogously for $\mathcal{I}_{[s,e]}^a$. We refer to $\|\cdot\|_{\mathcal{I}^d}$, $\|\cdot\|_{\mathcal{I}^a}$ and their restrictions as multiresolution sup-norms (see Nemirovski (1986) and Li (2016)) or, alternatively, multiscale scan statistics if they are used as operations on data. If the context requires this, the qualifier “dyadic” will be added to these terms when referring to the \mathcal{I}^d versions. The facts that, for any interval $[s, e]$ and any input vector y (of length T), we have

$$\|y_{s:e}\|_{\mathcal{I}_{[s,e]}^d} \leq \|y_{s:e}\|_{\mathcal{I}_{[s,e]}^a} \leq \|y\|_{\mathcal{I}^a} \quad \text{and} \quad \|y_{s:e}\|_{\mathcal{I}_{[s,e]}^d} \leq \|y\|_{\mathcal{I}^d} \leq \|y\|_{\mathcal{I}^a} \quad (4)$$

are trivial consequences of the facts that $\mathcal{I}_{[s,e]}^d \subseteq \mathcal{I}_{[s,e]}^a \subseteq \mathcal{I}^a$ and $\mathcal{I}_{[s,e]}^d \subseteq \mathcal{I}^d \subseteq \mathcal{I}^a$. With this notation in place, $\text{DEVIATIONFROMLINEARITY}(s_m, e_m, Y, X)$ is defined as follows.

Step 1. Find $\beta_0 = \arg \min_{\beta} \|Y_{s_m:e_m} - X_{s_m:e_m, \cdot} \beta\|_{\mathcal{I}_{[s_m, e_m]}^d}$. This fits the postulated linear model between X and Y restricted to the interval $[s_m, e_m]$. However, we use the multiresolution sup-norm $\|\cdot\|_{\mathcal{I}_{[s_m, e_m]}^d}$ as the loss function, rather than the more usual L_2 loss. This has important consequences for the exactness of our significance statements, which we explain later below.

Step 2. Compute the same multiresolution sup-norm of the empirical residuals from the above fit, $D_{[s_m, e_m]} := \|Y_{s_m:e_m} - X_{s_m:e_m, \cdot} \beta_0\|_{\mathcal{I}_{[s_m, e_m]}^d}$.

Step 3. Return $D_{[s_m, e_m]}$.

Steps 1. and 2. above can be carried out in a single step as $D_{[s_m, e_m]} = \min_{\beta} \|Y_{s_m:e_m} - X_{s_m:e_m, \cdot} \beta\|_{\mathcal{I}_{[s_m, e_m]}^d}$, however, for comparison with other approaches, it will be convenient for us to use the two-stage process in steps 1. and 2. for the computation of $D_{[s_m, e_m]}$. Computationally, the linear model fit in step 1. can be carried out via simple linear programming; we use the R package `lpSolve`. The following important property lies at the heart of NSP.

Proposition 2.1 *Let the interval $[s, e]$ be such that $\forall j = 1, \dots, N$ $[\eta_j, \eta_j + 1] \not\subseteq [s, e]$. We have $D_{[s,e]} \leq \|Z_{s:e}\|_{\mathcal{I}_{[s,e]}^d}$.*

This is a simple but valuable result, which can be read as follows: “under the local null hypothesis of no signal on $[s, e]$, the test statistic $D_{[s, e]}$, defined as the multiresolution sup-norm of the empirical residuals from the same multiresolution sup-norm fit of the postulated linear model on $[s, e]$, is bounded by the multiresolution sup-norm of the true residual process Z_t ”. This bound is achieved because the same norm is used in the linear model fit and in the residual check, and it is important to note that the corresponding bound would not be available if the postulated linear model were fitted with a different loss function, e.g. via OLS. Having such a bound allows us to transfer our statistical significance calculations to the domain of the unobserved true residuals Z_t , which is much easier than working with the corresponding empirical residuals. It is also critical to obtaining global coverage guarantees for NSP, as we now show.

Theorem 2.1 *Let $\mathcal{S} = \{S_1, \dots, S_R\}$ be a set of intervals returned by the NSP algorithm. We have $P(\exists i = 1, \dots, R \ \forall j = 1, \dots, N \ [\eta_j, \eta_j + 1] \not\subseteq S_i) \leq P(\|Z\|_{\mathcal{I}^d} > \lambda_\alpha) \leq P(\|Z\|_{\mathcal{I}^a} > \lambda_\alpha)$.*

Theorem 2.1 should be read as follows. Let $\alpha = P(\|Z\|_{\mathcal{I}^a} > \lambda_\alpha)$. For a set of intervals returned by NSP, we are guaranteed, with probability of at least $1 - \alpha$, that there is at least one change-point in each of these intervals. Therefore, $\mathcal{S} = \{S_1, \dots, S_R\}$ can be interpreted as an automatically chosen set of regions (intervals) of significance in the data. In the no-change-point case ($N = 0$), the correct reading of Theorem 2.1 is that the probability of obtaining one or more intervals of significance ($R \geq 1$) is bounded from above by $P(\|Z\|_{\mathcal{I}^a} > \lambda_\alpha)$.

NSP uses a multiresolution sup-norm fit to be checked via the same multiresolution sup-norm. This leads to exact coverage guarantees for NSP with very simple mathematics. In contrast to the confidence intervals in e.g. Bai and Perron (1998), the NSP regions of significance are not conditional on any particular estimator of N , and are in addition of a finite-sample nature. Still, they have a “confidence interval” interpretation in the sense that each must contain at least one change, with a certain prescribed global probability.

For $S_i = [s, e]$, we define $S_i^- = [s, e - 1]$. A simple corollary of Theorem 2.1 is that for

$\mathcal{S} = \{S_1, \dots, S_R\}$, if the corresponding sets S_i^- are mutually disjoint (as is the case e.g. if $\tau_L = \tau_R \equiv 0$), then we must have $N \geq R$ with probability at least $1 - \alpha$. It would be impossible to obtain a similar upper bound on N without order-of-magnitude assumptions on spacings between change-points and magnitudes of parameter changes; we defer this to Section 4. The result in Theorem 2.1 does not rely on asymptotics and has a finite-sample character.

β_0 in Step 1 above does not have to be an accurate estimator of the true local β for the bound in Proposition 2.1 to hold; it holds unconditionally and for arbitrary short intervals $[s, e]$. This is in contrast to e.g. an OLS fit, in which we would have to ensure accurate estimation of the local β (and therefore: suitably long intervals $[s, e]$) to be able to obtain similar bounds. We return to this important issue in Section 3.2.

NSP is not automatically equipped with pointwise estimators of change-point locations. This is an important feature, because thanks to this, it can be so general and work in the same way for any X without a change. If it were to come with meaningful pointwise change-point location estimators, they would have to be designed for each X separately, e.g. using the maximum likelihood principle. (However, NSP can be paired up with such pointwise estimators; see below for details.) We now introduce a few new concepts, to contrast this feature of NSP with the existing concept of post-selection inference.

“Post-inference selection” and “inference without selection”. If it can be assumed that an interval $S_i = [s_i, e_i] \in \mathcal{S}$ only contains a single change-point, its location can be estimated e.g. via MLE performed locally on the data subsample living on $[s_i, e_i]$. Naturally, the MLE should be constructed with the specific design matrix X in mind, see Baranowski et al. (2019) for examples in Scenarios 1 and 2. In this construction, “inference”, i.e. the execution of NSP, occurs before “selection”, i.e. the estimation of the change-point locations, hence the label of “post-inference selection”. This avoids the complicated machinery of post-selection inference, as we automatically know that the p -value associated with the estimated change-point must be less than α . Similarly, “inference without selection” refers to the use of NSP unaccompanied by a change-point location estimator.

“*Simultaneous inference and selection*” or “*in-inference selection*”. In this construction, change-point location estimation on an interval $[\tilde{s}, \tilde{e}]$ occurs directly after adding it to \mathcal{S} . The difference with “post-inference selection” is that this then naturally enables appropriate non-zero overlaps τ_L and τ_R in the execution of NSP. More specifically, denoting the estimated location within $[\tilde{s}, \tilde{e}]$ by $\tilde{\eta}$, we can set, for example, $\tau_L(\tilde{s}, \tilde{e}, Y, X) = \tilde{\eta} - \tilde{s}$ and $\tau_R(\tilde{s}, \tilde{e}, Y, X) = \tilde{e} - \tilde{\eta} - 1$, so that lines 21–22 of the NSP algorithm become, respectively, $\text{NSP}(s, \tilde{\eta}, Y, X, M, \lambda_\alpha, \tau_L, \tau_R)$ and $\text{NSP}(\tilde{\eta} + 1, e, Y, X, M, \lambda_\alpha, \tau_L, \tau_R)$.

By Theorem 2.1, the only piece of knowledge required to obtain coverage guarantees in NSP is the distribution of $\|Z\|_{\mathcal{I}^a}$ (or $\|Z\|_{\mathcal{I}^d}$), regardless of the form of X . Much is known about this distribution for various underlying distributions of Z ; see Section 2.3 below and Section D of the appendix for Z Gaussian and following other light-tailed distributions, respectively. Any future further distributional results of this type would only further enhance the applicability of NSP. However, if the distribution of $\|Z\|_{\mathcal{I}^a}$ ($\|Z\|_{\mathcal{I}^d}$) is unknown, then an approximation can also be obtained by simulation, which is particularly computationally efficient for $\|Z\|_{\mathcal{I}^d}$.

2.3 $Z_t \sim \text{i.i.d. } N(0, \sigma^2)$

We now recall distributional results for $\|Z\|_{\mathcal{I}^a}$, in the case $Z_t \sim \text{i.i.d. } N(0, \sigma^2)$ with σ^2 assumed known, which will permit us to choose $\lambda_\alpha = \lambda_\alpha(T)$ so that $P\{\|Z\|_{\mathcal{I}^a} > \lambda_\alpha(T)\} \rightarrow \alpha$ as $T \rightarrow \infty$. The resulting $\lambda_\alpha(T)$ can then be used in Theorem 2.1. As the result of Theorem 2.1 is otherwise of a finite-sample nature, some users may be uncomfortable resorting to large-sample asymptotics to approximate the distribution of $\|Z\|_{\mathcal{I}^a}$. However, (a) the asymptotic results outlined below approximate the behaviour of $\|Z\|_{\mathcal{I}^a}$ well even for small samples, and (b) users not wishing to resort to asymptotics have the option of approximating the distribution of $\|Z\|_{\mathcal{I}^a}$ by simulation, which is computationally fast.

The assumption of a known σ^2 is common in the change-point inference literature, see e.g. Hyun et al. (2018), Fang and Siegmund (2020) and Jewell et al. (2022). Section D of the appendix covers the unknown σ^2 case; we show there a condition under which Theorem 2.2

remains valid with an estimated variance σ^2 , and give an estimator of σ^2 that satisfies that condition for certain matrices X and parameter vectors $\beta^{(j)}$.

Results on the distribution of $\|Z\|_{\mathcal{I}^a}$ are given in Siegmund and Venkatraman (1995) and Kabluchko (2007). We recall the formulation from Kabluchko (2007) as it is slightly more explicit.

Theorem 2.2 (Theorem 1.3 in Kabluchko (2007)) *Let $\{Z_t\}_{t=1}^T$ be i.i.d. $N(0, 1)$. For every $\gamma \in \mathbb{R}$, we have $\lim_{T \rightarrow \infty} P(\max_{1 \leq s \leq e \leq T} U_{s,e}(Z) \leq a_T + b_T \gamma) = \exp(-e^{-\gamma})$, where*

$$a_T = \sqrt{2 \log T} + \frac{\frac{1}{2} \log \log T + \log \frac{H}{2\sqrt{\pi}}}{\sqrt{2 \log T}}; \quad b_T = \frac{1}{\sqrt{2 \log T}}; \quad H = \int_0^\infty \exp\left(-4 \sum_{k=1}^\infty \frac{1}{k} \Phi\left(-\sqrt{\frac{k}{2y}}\right)\right) dy,$$

and $\Phi()$ is the standard normal cdf.

We use the approximate value $H = 0.82$ in our numerical work. Using the asymptotic independence of the maximum and the minimum (Kabluchko and Wang, 2014), and the symmetry of Z , we get the following simple corollary.

$$\begin{aligned} P\left(\max_{1 \leq s \leq e \leq T} |U_{s,e}(Z)| > a_T + b_T \gamma\right) &= 1 - P\left(\max_{1 \leq s \leq e \leq T} |U_{s,e}(Z)| \leq a_T + b_T \gamma\right) = \\ &= 1 - P\left(\max_{1 \leq s \leq e \leq T} U_{s,e}(Z) \leq a_T + b_T \gamma \quad \wedge \quad \min_{1 \leq s \leq e \leq T} U_{s,e}(Z) \geq -(a_T + b_T \gamma)\right) \rightarrow \\ &= 1 - \exp(-2e^{-\gamma}) \end{aligned} \tag{5}$$

as $T \rightarrow \infty$. In light of (5), we obtain λ_α for use in Theorem 2.1 as follows: (a) equate $\alpha = 1 - \exp(-2e^{-\gamma})$ and obtain γ , (b) form $\lambda_\alpha = \sigma(a_T + b_T \gamma)$.

3 NSP with self-normalisation and with autoregression

3.1 Self-normalised NSP for possibly heavy-tailed, heteroscedastic Z_t

Kabluchko and Wang (2014) point out that the square-root normalisation used in $U_{s,e}(y)$ is not natural for distributions with tails heavier than Gaussian. We are interested in obtaining a universal normalisation in $U_{s,e}(y)$ which would work across a wide range of possibly

heavy-tailed distributions without requiring their explicit knowledge, including under heterogeneity. One such solution is offered by the self-normalisation framework developed in Račkauskas and Suquet (2003) and related papers. We now recall the basics and discuss the necessary adaptations to our context. We first discuss the relevant distributional results for the true residuals Z_t . In this paper, we only cover the case of symmetric distributions of Z_t . For the non-symmetric case, which requires a slightly different normalisation, see Račkauskas and Suquet (2003). In Račkauskas and Suquet (2003), the following result is proved. Let $\rho_{\theta,\nu,c}(\delta) = \delta^\theta \log^\nu(c/\delta)$, $0 < \theta < 1$, $\nu \in \mathbb{R}$, where $c \geq \exp(\nu/\theta)$ if $\nu > 0$ and $c > \exp(-\nu/(1-\theta))$ if $\nu < 0$. Further, suppose $\lim_{j \rightarrow \infty} 2^j \rho_{\theta,\nu,c}^2(2^{-j})/j = \infty$. This last condition, in particular, is satisfied if $\theta = 1/2$ and $\nu > 1/2$. The function $\rho_{\theta,\nu,c}$ will play the role of a modulus of continuity. Let Z_1, Z_2, \dots be independent and symmetrically distributed with $\mathbb{E}(Z_t) = 0$; note they do not need to be identically distributed. Define $S_t = Z_1 + \dots + Z_t$ and $V_t^2 = Z_1^2 + \dots + Z_t^2$. Assume further $V_T^{-2} \max_{1 \leq t \leq T} Z_t^2 \rightarrow 0$ in probability as $T \rightarrow \infty$. Egorov (1997) shows that this last condition is equivalent to Z_t being within the domain of attraction of the normal law. Therefore, the material of this section applies to a much wider class of distributions than the heterogeneous extension of SMUCE in Pein et al. (2017), which only applies to normally distributed Z_t .

Let the random polygonal partial sums process ζ_T be defined on $[0, 1]$ as linear interpolation between the knots $(V_t^2/V_T^2, S_t)$, $t = 0, \dots, T$, where $S_0 = V_0 = 0$, and let $\zeta_T^{\text{se}} = \zeta_T/V_T$. Denote by $H_{\rho_{\theta,\nu,c}}[0, 1]$ the set of continuous functions $x : [0, 1] \rightarrow \mathbb{R}$ such that $\omega_{\rho_{\theta,\nu,c}}(x, 1) < \infty$, where $\omega_{\rho_{\theta,\nu,c}}(x, \delta) = \sup_{u,v \in [0,1], 0 < |v-u| < \delta} |x(v) - x(u)|/\rho_{\theta,\nu,c}(|v-u|)$. $H_{\rho_{\theta,\nu,c}}[0, 1]$ is a Banach space in its natural norm $\|x\|_{\rho_{\theta,\nu,c}} = |x(0)| + \omega_{\rho_{\theta,\nu,c}}(x, 1)$. Define $H_{\rho_{\theta,\nu,c}}^0[0, 1]$, a closed subspace of $H_{\rho_{\theta,\nu,c}}[0, 1]$, by $H_{\rho_{\theta,\nu,c}}^0[0, 1] = \{x \in H_{\rho_{\theta,\nu,c}}[0, 1] : \lim_{\delta \rightarrow 0} \omega_{\rho_{\theta,\nu,c}}(x, \delta) = 0\}$. $H_{\rho_{\theta,\nu,c}}^0[0, 1]$ is a separable Banach space. Under the assumptions above, we have the following convergence in distribution as $T \rightarrow \infty$:

$$\zeta_T^{\text{se}} \rightarrow W \tag{6}$$

in $H_{\rho_{\theta,\nu,c}}^0[0, 1]$, where $W(u)$, $u \in [0, 1]$ is a standard Wiener process. Define $I_{\rho_{\theta,\nu,c}}(x, u, v) =$

$|x(v) - x(u)|/\rho_{\theta,\nu,c}(|v - u|)$ and, with $\epsilon > 0$ and $c = \exp(1 + 2\epsilon)$, consider the statistic

$$\begin{aligned} \sup_{0 \leq i < j \leq T} I_{\rho_{1/2,1/2+\epsilon,c}}(\zeta_T^{\text{se}}, V_i^2/V_T^2, V_j^2/V_T^2) &= \sup_{0 \leq i < j \leq T} \frac{|\zeta_T^{\text{se}}(V_j^2/V_T^2) - \zeta_T^{\text{se}}(V_i^2/V_T^2)|}{\rho_{1/2,1/2+\epsilon,c}(V_j^2/V_T^2 - V_i^2/V_T^2)} = \\ &= \sup_{0 \leq i < j \leq T} \frac{|S_j - S_i|}{\sqrt{V_j^2 - V_i^2} \log^{1/2+\epsilon}\{c/(V_j^2/V_T^2 - V_i^2/V_T^2)\}} = \\ &= \sup_{0 \leq i < j \leq T} \frac{|Z_{i+1} + \dots + Z_j|}{\sqrt{Z_{i+1}^2 + \dots + Z_j^2} \log^{1/2+\epsilon}\{cV_T^2/(Z_{i+1}^2 + \dots + Z_j^2)\}}. \end{aligned}$$

In the notation and under the conditions listed above, it is a direct consequence of the distributional convergence (6) in the space $H_{\rho_{\theta,\nu,c}}^0[0,1]$ that for any level γ , we have

$$\begin{aligned} P\left(\sup_{0 \leq i < j \leq T} I_{\rho_{1/2,1/2+\epsilon,c}}(\zeta_T^{\text{se}}, V_i^2/V_T^2, V_j^2/V_T^2) \geq \gamma\right) &\leq \\ P\left(\sup_{u,v \in [0,1]} I_{\rho_{1/2,1/2+\epsilon,c}}(\zeta_T^{\text{se}}, u, v) \geq \gamma\right) &\rightarrow P\left(\sup_{u,v \in [0,1]} I_{\rho_{1/2,1/2+\epsilon,c}}(W, u, v) \geq \gamma\right) \quad (7) \end{aligned}$$

as $T \rightarrow \infty$, and the quantiles of the distribution of $\sup_{u,v \in [0,1]} I_{\rho_{1/2,1/2+\epsilon,c}}(W, u, v)$, which does not depend on the sample size T , can be computed (once) by simulation.

Following the narrative of Sections 2.2 and 2.3, to make these results operational in a new function `DEVIATIONFROMLINEARITY.SN` (where ‘SN’ stands for self-normalisation), to replace the function `DEVIATIONFROMLINEARITY` in line 12 of the NSP algorithm, we need the following development. Assume initially that the global residual sum of squares V_T^2 is known. For a generic interval $[s, e]$ containing no change-points, we need to be able to obtain empirical residuals $\hat{Z}_{i+1}^{(k)}, \dots, \hat{Z}_j^{(k)}$ for $k = 1, 2$ and $\hat{Z}_s^{(k)}, \dots, \hat{Z}_e^{(k)}$ for $k = 3$ for which we can guarantee that

$$\begin{aligned} \sup_{s-1 \leq i < j \leq e} \frac{|\hat{Z}_{i+1}^{(3)} + \dots + \hat{Z}_j^{(3)}|}{\sqrt{(\hat{Z}_{i+1}^{(2)})^2 + \dots + (\hat{Z}_j^{(2)})^2} \log^{1/2+\epsilon}\{cV_T^2/((\hat{Z}_{i+1}^{(1)})^2 + \dots + (\hat{Z}_j^{(1)})^2)\}} &\leq \\ \sup_{s-1 \leq i < j \leq e} \frac{|Z_{i+1} + \dots + Z_j|}{\sqrt{Z_{i+1}^2 + \dots + Z_j^2} \log^{1/2+\epsilon}\{cV_T^2/(Z_{i+1}^2 + \dots + Z_j^2)\}} &\quad (8) \end{aligned}$$

Section F of the appendix describes in detail the construction of $\hat{Z}^{(k)}$ for $k = 1, 2, 3$ so that (8) is guaranteed, and introduces a suitable estimator of V_T^2 for use in (8).

3.2 NSP with autoregression

To accommodate autoregression, we introduce the following additional scenario.

Scenario 4. *Linear regression with autoregression, with piecewise-constant parameters.*

For a given design matrix $X = (X_{t,i})$, $t = 1, \dots, T$, $i = 1, \dots, p$, the response Y_t follows the model

$$Y_t = X_{t,\cdot} \beta^{(j)} + \sum_{k=1}^r a_k^{(j)} Y_{t-k} + Z_t \quad \text{for } t = \eta_j + 1, \dots, \eta_{j+1}, \quad (9)$$

for $j = 0, \dots, N$, where the regression parameter vectors $\beta^{(j)} = (\beta_1^{(j)}, \dots, \beta_p^{(j)})'$ and the autoregression parameters $a_k^{(j)}$ are such that either $\beta^{(j)} \neq \beta^{(j+1)}$ or $a_k^{(j)} \neq a_k^{(j+1)}$ for some k (or both types of changes occur).

In this work, we treat the autoregressive order r as fixed and known to the analyst. Change-point detection in the signal in the presence of serial correlation is a well-known challenging problem in change-point analysis and many methods (see e.g. Dette et al. (2020) for an example and a literature review) rely on the accurate estimation of the long-run variance of the noise, a difficult problem. Fang and Siegmund (2020) consider $r = 1$ and treat the autoregressive parameter as known, but acknowledge that in practice it is estimated from the data; however, they add that “[it] would also be possible to estimate [the autoregressive parameter] from the currently studied subset of the data, but this estimator appears to be unstable”. NSP circumvents this instability issue, as explained below. NSP for Scenario 4 proceeds as follows.

1. Supplement the design matrix X with the lagged versions of the variable Y , or in other words substitute $X := \begin{bmatrix} X & Y_{-1} & \dots & Y_{-r} \end{bmatrix}$, where Y_{-k} denotes the respective backshift operation. Omit the first r rows of the thus-modified X , and the first r elements of Y .
2. Run the NSP algorithm of Section 2.1 with the new X and Y (with a suitable modification to line 12 if using the self-normalised version), with the following single

difference. In lines 21 and 22, recursively call the NSP routine on the intervals $[s, \tilde{s} + \tau_L(\tilde{s}, \tilde{e}, Y, X) - r]$ and $[\tilde{e} - \tau_R(\tilde{s}, \tilde{e}, Y, X) + r, e]$, respectively. As each local regression is now supplemented with autoregression of order r , we insert the extra “buffer” of size r between the detected interval $[\tilde{s}, \tilde{e}]$ and the next children intervals to ensure that we do not process information about the same change-point in both the parent call and one of the children calls, which prevents double detection.

As the NSP algorithm for Scenario 4 proceeds in exactly the same way as for Scenario 3, the result of Theorem 2.1 applies to the output of NSP for Scenario 4 too. The NSP algorithm offers a new point of view on change-point analysis in the presence of autocorrelation. This is because unlike the existing approaches, most of which require the accurate estimation of the autoregressive parameters before successful change-point detection can be achieved, NSP circumvents the issue by using the same multiresolution norm in the local regression fits on each $[s, e]$, and in the subsequent tests of the local residuals. In this way, the autoregression parameters do not have to be estimated accurately for the relevant stochastic bound in Proposition 2.1 to hold; it holds unconditionally and for arbitrary short intervals $[s, e]$. Therefore unlike e.g. the method of Fang and Siegmund (2020), NSP is able to deal with autoregression, stably, on arbitrarily short intervals.

4 Detection consistency and lengths of NSP intervals

This section shows the consistency of NSP in detecting change-points, and the rates at which the lengths of the NSP intervals contract, as the sample size increases. To simplify the exposition, we consider a version of the NSP algorithm that considers all sub-intervals of $[1, T]$, and we provide results in Scenario 1 as well as in Scenario 2 with continuous piecewise-linearity (this parallels the scenarios for which consistency is shown in Baranowski et al. (2019)).

So far in the paper, we avoided introducing any assumptions on the signal: our coverage guarantees in Theorem 2.1 held under no conditions on the number of change-points, their spacing, or the sizes of the breaks. This was unsurprising as they amounted to statistical size

control. By contrast, the results of this section relate to detection consistency (and therefore ‘power’ rather than size) and as such, require minimum signal strength assumptions.

4.1 Scenario 1 – piecewise constancy

In this section, f_t falls under Scenario 1. We start with assumptions on the strength of the change-points. For each change-point η_j , $j = 1, \dots, N$, define

$$\bar{d}_j = \left\lceil \frac{16\lambda_\alpha^2}{|f_{\eta_{j+1}} - f_{\eta_j}|^2} \right\rceil + 1. \quad (10)$$

Recalling that $\eta_0 = 0$ and $\eta_{N+1} = T$, we require the following assumption.

Assumption 4.1 $\eta_{j+1} - \eta_j \geq 2\bar{d}_{j+1} + 2\bar{d}_j - 2$ ($j = 1, \dots, N - 1$); $\eta_1 - \eta_0 \geq 2\bar{d}_1 - 1$; $\eta_{N+1} - \eta_N \geq 2\bar{d}_N - 1$.

We have the following theorem.

Theorem 4.1 *Let Assumption 4.1 hold, with \bar{d}_j defined in (10). On the set $\|Z\|_{\mathcal{I}^a} \leq \lambda_\alpha$, a version of the NSP algorithm that considers all sub-intervals, executed with no overlaps and with threshold λ_α , returns exactly N intervals of significance $[s_1, e_1] < \dots < [s_N, e_N]$ such that $\eta_j \in [s_j, e_j - 1]$ and $e_j - s_j + 1 \leq 2\bar{d}_j$, for $j = 1, \dots, N$.*

Theorem 4.1 leads to the following corollary.

Corollary 4.1 *Let the assumptions of Theorem 4.1 hold, and in addition let $Z_t \sim N(0, \sigma^2)$. Let $\lambda_\alpha = \sigma(1 + \Delta)\sqrt{2\log T}$ for any $\Delta > 0$. Let \mathcal{S} denote the set of intervals of significance $[s_1, e_1] < [s_2, e_2] < \dots$ returned by a version of the NSP algorithm that considers all sub-intervals, executed with no overlaps and with threshold λ_α . Let $\mathcal{A} = \{|\mathcal{S}| = N \wedge \forall j = 1, \dots, N \ \eta_j \in [s_j, e_j - 1] \wedge e_j - s_j + 1 \leq 2\bar{d}_j\}$. We have $P(\mathcal{A}) \rightarrow 1$ as $T \rightarrow \infty$.*

Corollary 4.1 is a traditional, large-sample consistency result for NSP. Consider first Assumption 4.1, under which it operates. With λ_α as in Corollary 4.1, Assumption 4.1 permits $\min_j \{|\eta_{j+1} - \eta_j|^{1/2} \min(|f_{\eta_{j+1}} - f_{\eta_j}|, |f_{\eta_{j+1}+1} - f_{\eta_{j+1}}|)\}$, a quantity that characterises the

difficulty of the multiple change-point detection problem, to be of order $O(\log^{1/2} T)$, which is the same as in Baranowski et al. (2019) and minimax-optimal as argued in Chan and Walther (2013). Further, the statement of Corollary 4.1 implies statistical consistency of NSP in the sense that with probability tending to one with T , NSP estimates the correct number of change-points and each NSP interval contains exactly one true change-point. Moreover, the length of the NSP interval around each η_j is of order $O(\log T/|f_{\eta_j+1} - f_{\eta_j}|^2)$, which is near-optimal and the same as in Baranowski et al. (2019). Finally, this also implies that this consistency rate is inherited by *any* pointwise estimator of η_j that takes its value in the j th NSP interval of significance; this applies even to naive estimators constructed e.g. as the middle points of their corresponding NSP intervals $[s_j, e_j]$, i.e. $\hat{\eta}_j = \lfloor (s_j + e_j)/2 \rfloor$. More refined estimators, e.g. one based on CUSUM maximisation within each NSP interval, can also be used and they will also automatically inherit the consistency and rate.

4.2 Scenario 2 – continuous piecewise linearity

In this section, f_t falls under Scenario 2 and is piecewise linear and continuous. Naturally, the definition of change-point strength has to be different from that in Section 4.1. For each change-point η_j , $j = 1, \dots, N$, let

$$\bar{d}_j = \left\lceil C_2 \lambda_\alpha^{2/3} \xi_j^{-2/3} \right\rceil, \quad (11)$$

where $\xi_j = |\xi_{j,1} - \xi_{j,2}|/2$ and $\xi_{j,1}, \xi_{j,2}$ are, respectively, the slopes of f_t immediately to the left and to the right of η_j , and C_2 is a certain universal constant (i.e. valid for all f_t), suitably large. The following theorem holds.

Theorem 4.2 *Let Assumption 4.1 hold, with \bar{d}_j defined in (11). On the set $\|Z\|_{\mathcal{I}^a} \leq \lambda_\alpha$, a version of the NSP algorithm that considers all sub-intervals, executed with no overlaps and with threshold λ_α , returns exactly N intervals of significance $[s_1, e_1] < \dots < [s_N, e_N]$ such that $\eta_j \in [s_j, e_j - 1]$ and $e_j - s_j + 1 \leq 2\bar{d}_j$, for $j = 1, \dots, N$.*

We note that Assumption 4.1 is model-independent: we require it as much in the piecewise-constant Scenario 1 as in the piecewise-linear Scenario 2 (and in any other scenario), but

with \bar{d}_j defined separately for each scenario. Theorem 4.2 leads to the following corollary.

Corollary 4.2 *Let the assumptions of Theorem 4.2 hold, and in addition let $Z_t \sim N(0, \sigma^2)$. Let $\lambda_\alpha = \sigma(1 + \Delta)\sqrt{2\log T}$ for any $\Delta > 0$. Let \mathcal{S} denote the set of intervals of significance $[s_1, e_1] < [s_2, e_2] < \dots$ returned by a version of the NSP algorithm that considers all sub-intervals, executed with no overlaps and with threshold λ_α . Let $\mathcal{A} = \{|\mathcal{S}| = N \wedge \forall j = 1, \dots, N \ \eta_j \in [s_j, e_j - 1] \wedge e_j - s_j + 1 \leq 2\bar{d}_j\}$. We have $P(\mathcal{A}) \rightarrow 1$ as $T \rightarrow \infty$.*

Corollary 4.2 implies that with λ_α as defined therein, and if $\xi_j \sim T^{-1}$ (a case in which f_t is bounded; see Baranowski et al. (2019)), we have that the accuracy of change-point localisation via NSP (measured by $e_j - s_j$) is $O(T^{2/3} \log^{1/3} T)$, the same as in Baranowski et al. (2019) and within a logarithmic factor of Raimondo (1998). Our comment (made in Section 4.1) regarding this rate being inherited by any pointwise estimator of η_j , as long as it falls within $[s_j, e_j]$, applies equally in this case.

5 Numerical illustrations

In addition to the settings below, the appendix contains further examples.

5.1 Scenario 1 – piecewise constancy

5.1.1 Low signal-to-noise example

We use the piecewise-constant `blocks` signal of length $T = 2048$ containing $N = 11$ change-points, defined in Fryzlewicz (2014). We add i.i.d. Gaussian noise with $\sigma = 10$, simulated with random seed set to 1. This represents a difficult setting for multiple change-point detection, with practically all state of the art multiple change-point detection methods failing to estimate all 11 change-points with high probability (Anastasiou and Fryzlewicz, 2022). Therefore, a high degree of uncertainty with regards to the existence and locations of change-points can be expected here.

The NSP procedure with the $\hat{\sigma}_{MAD}$ estimate of σ , run with the following parameters: $M = 1000$, $\alpha = 0.1$, $\tau_L = \tau_R = 0$, and with a deterministic interval sampling grid, returns

7 intervals of significance, shown in the top left plot of Figure 1. We recall that at a fixed significance level, it is not the aim of the NSP procedure to detect all change-points. The correct interpretation of the result is that we can be at least $100(1 - \alpha)\% = 90\%$ certain that each of the intervals returned by NSP covers at least one true change-point. We note that this coverage holds for this particular sample path, with exactly one true change-point being located within each interval of significance.

NSP enables the following definition of a change-point hierarchy. A hypothesised change-point contained in the detected interval of significance $[\tilde{s}_1, \tilde{e}_1]$ is considered more prominent than one contained in $[\tilde{s}_2, \tilde{e}_2]$ if $[\tilde{s}_1, \tilde{e}_1]$ is shorter than $[\tilde{s}_2, \tilde{e}_2]$. The bottom left plot of Figure 1 shows a “prominence plot” for this output of the NSP procedure, in which the lengths of the detected intervals of significance are arranged in the order from the shortest to the longest.

It is unsurprising that the intervals returned by NSP do not cover the remaining 4 change-points, as from a visual inspection, it appears that all of them are located towards the edges of data sections situated between the intervals of significance. Executing NSP without an overlap, i.e. with $\tau_L = \tau_R = 0$, means that the procedure runs, in each recursive step, wholly on data sections between (and only including the end-points of) the previously detected intervals of significance. Therefore, in light of the close-to-the-edge locations of the remaining 4 change-points within such data sections, and the low signal-to-noise ratio, any procedure would struggle to detect them there.

This shows the importance of allowing non-zero overlaps τ_L and τ_R in NSP. We try the following.

$$\tau_L(\tilde{s}, \tilde{e}) = \lfloor (\tilde{s} + \tilde{e})/2 \rfloor - \tilde{s}; \quad \tau_R(\tilde{s}, \tilde{e}) = \lfloor (\tilde{s} + \tilde{e})/2 \rfloor + 1 - \tilde{e}. \quad (12)$$

This setting means that upon detecting a generic interval of significance $[\tilde{s}, \tilde{e}]$ within $[s, e]$, the NSP algorithm continues on the left interval $[s, \lfloor (\tilde{s} + \tilde{e})/2 \rfloor]$ and the right interval $[\lfloor (\tilde{s} + \tilde{e})/2 \rfloor + 1, e]$ (recall that the no-overlap case results uses the left interval $[s, \tilde{s}]$ and the right interval $[\tilde{e}, e]$). The outcome of the NSP procedure with the overlap functions in (12) but otherwise the same parameters as earlier is shown in the top right plot of Figure 1.

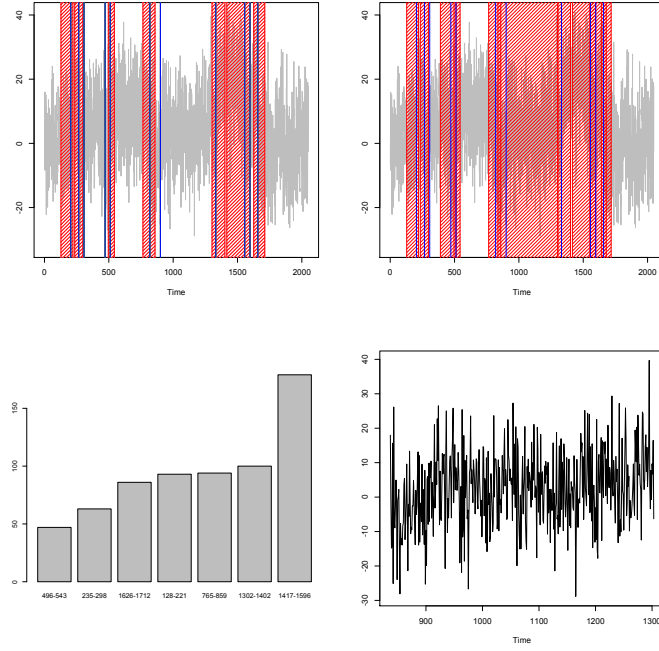


Figure 1: Top left: realisation Y_t of noisy **blocks** with $\sigma = 10$ (light grey), true change-point locations (blue), NSP intervals of significance ($\alpha = 0.1$) with no overlap (shaded red). Top right: the same but with overlap as in (12). Bottom left: “prominence plot” – bar plot of $\tilde{e}_i - \tilde{s}_i$, $i = 1, \dots, 7$, plotted in increasing order, where $[\tilde{s}_i, \tilde{e}_i]$ are the NSP no-overlap significance intervals; the labels are “ $\tilde{s}_i - \tilde{e}_i$ ”. Bottom right: $Y_{837:1303}$. See Section 5.1.1 for more details.

This version of the procedure returns 10 intervals of significance, such that (a) each interval covers at least one true change-point, and (b) they collectively cover 10 of the signal’s $N = 11$ change-points, the only exception being $\eta_3 = 307$.

We briefly remark that one of the returned intervals of significance, $[\tilde{s}, \tilde{e}] = [837, 1303]$, is much longer than the others, but this should not surprise given that the (only) change-point it covers, $\eta_7 = 901$, is barely, if at all, suggested by the visual inspection of the data. The data section $Y_{837:1303}$ is shown in the bottom right plot of Figure 1.

Finally, we mention computation times for this particular example, on a standard 2015 iMac: 14 seconds ($M = 1000$, no overlap), 24 seconds ($M = 1000$, overlap as above), 1.6 seconds ($M = 100$, no overlap), and 2.6 seconds ($M = 100$, overlap as above).

5.1.2 NSP vs SMUCE: coverage comparison

For the NSP procedure, Theorem 2.1 promises that the probability of detecting an interval of significance which does not cover a true change-point is bounded from above by $P(\|Z\|_{\mathcal{I}^a} > \lambda_\alpha)$, regardless of the value of M and of the overlap parameters τ_L, τ_R . In this section, we set $P(\|Z\|_{\mathcal{I}^a} > \lambda_\alpha) = \alpha = 0.1$.

We now show that a similar coverage guarantee is not available in SMUCE, even if we move away from its focus on N as an inferential quality, thereby putting SMUCE through a more lenient performance test. In R, SMUCE is implemented in the package `stepR`, available from CRAN. For a generic data vector \mathbf{y} , the start- and end-points of the confidence intervals for the SMUCE-estimated change-point locations (at significance level $\alpha = 0.1$) are available in columns 3 and 4 of the table returned by the call `jumpint(stepFit(y, alpha=0.1, confband=T))` with the exception of its final row.

In this numerical example, we consider again the `blocks` signal with $\sigma = 10$. For each of 100 simulated sample paths, we record a “1” for SMUCE if each interval defined above contains at least one true change-point, and a “0” otherwise. Similarly, we record a “1” for NSP if each interval S_i^- contains at least one true change-point, where $\mathcal{S} = \{S_1, \dots, S_R\}$ is the set of intervals returned by NSP, and a “0” otherwise. As before, in NSP, we use $M = 1000$, $\tau_L = \tau_R = 0$, and a deterministic interval sampling grid.

With the random seed set to 1 prior to the simulation of the sample paths, the percentages of “1”’s obtained for SMUCE and NSP are: 52 and 100, respectively. While NSP (generously) keeps its promise of delivering a “1” with the probability of at least 0.9, the same cannot be said for SMUCE, for which the result of 52% makes the interpretation of its significance parameter $\alpha = 0.1$ difficult.

5.2 Scenario 2 – piecewise linearity

We consider the continuous, piecewise-linear `shortwave2` signal, defined as the first 450 elements of the `wave2` signal from Baranowski et al. (2019), contaminated with i.i.d. Gaussian noise with $\sigma = 0.5$. The signal and a sample path are shown in Figure 2. In this model, we

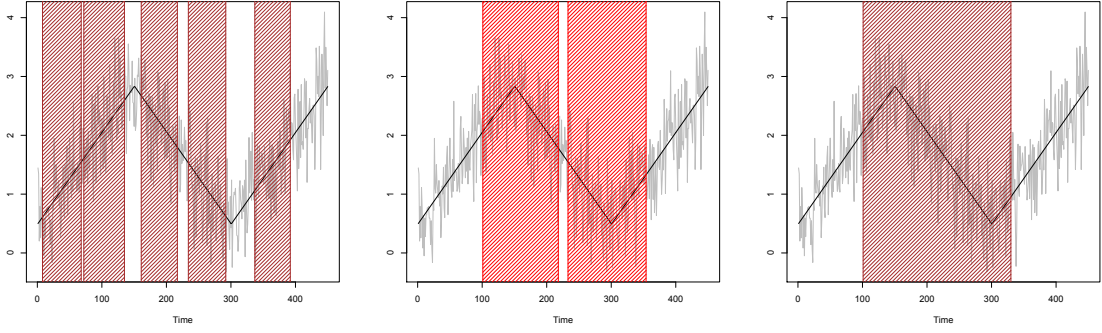


Figure 2: Noisy (light grey) and true (black) `shortwave2` signal, with NSP_q significance intervals for $q = 0$ (left, misspecified model), $q = 1$ (middle, well-specified model), $q = 2$ (right, over-specified model). See Section 5.2 for more details.

run the NSP procedure, with no overlaps and with the other parameters set as in Section 5.1.1, (wrongly or correctly) assuming the following, where q denotes the postulated degree of the underlying piecewise polynomial: (a) $q = 0$, which wrongly assumes that the true signal is piecewise constant; (b) $q = 1$, which assumes the correct degree of the polynomial pieces making up the signal; $q = 2$, which over-specifies the degree. We denote the result-versions of the NSP procedure by NSP_q for $q = 0, 1, 2$. The intervals of significance returned by all three NSP_q methods are shown in Figure 2. Theorem 2.1 guarantees that the NSP_1 intervals each cover a true change-point with probability of at least $1 - \alpha = 0.9$ and this behaviour occurs in this particular realisation. The same guarantee holds for the over-specified situation in NSP_2 , but there is no performance guarantee for NSP_0 .

The total length of the intervals of significance returned by NSP_q for a range of q can potentially be used to aid the selection of the ‘best’ q . To illustrate this potential use, note that the total length of the NSP_0 intervals of significance is much larger than that of NSP_1 or NSP_2 , and therefore the piecewise-constant model would not be preferred here on the grounds that the data deviates from it over a large proportion of its domain. The total lengths of the intervals of significance for NSP_1 and NSP_2 are very similar, and hence the piecewise-linear model might (correctly) be preferred here as offering a good description of a similar portion of the data, with fewer parameters than the piecewise-quadratic model.

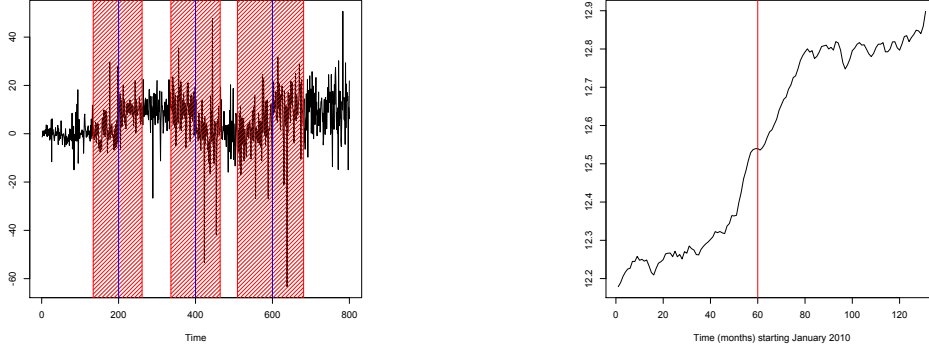


Figure 3: Left: **squarewave** signal with heterogeneous t_4 noise (black), self-normalised NSP intervals of significance (shaded red), true change-points (blue); see Section 5.3 for details. Right: time series Q_t for $t = 1, \dots, 131$. Red: the centre of the (single) NSP interval of significance. See Section 6.2 for details.

5.3 Self-normalised NSP

We briefly illustrate the performance of the self-normalised NSP. We define the piecewise-constant **squarewave** signal as taking the values of 0, 10, 0, 10, each over a stretch of 200 time points. With the random seed set to 1, we contaminate it with a sequence of independent t -distributed random variables with 4 degrees of freedom, with the standard deviation changing linearly from $\sigma_1 = 2\sqrt{2}$ to $\sigma_{800} = 8\sqrt{2}$. The simulated dataset, showing the “spiky” nature of the noise, is in the left plot of Figure 3.

We run the self-normalised version of NSP with the following parameters: a deterministic equispaced interval sampling grid, $M = 1000$, $\alpha = 0.1$, $\epsilon = 0.03$, no overlap; the outcome is in the left plot of Figure 3. Each true change-point is correctly contained within a (separate) NSP interval of significance, and we note that no spurious intervals get detected despite the heavy-tailed and heterogeneous character of the noise.

6 Data examples

6.1 The US ex-post real interest rate

We re-analyse the time series of US ex-post real interest rate (the three-month treasury bill rate deflated by the CPI inflation rate) considered in Garcia and Perron (1996) and Bai and

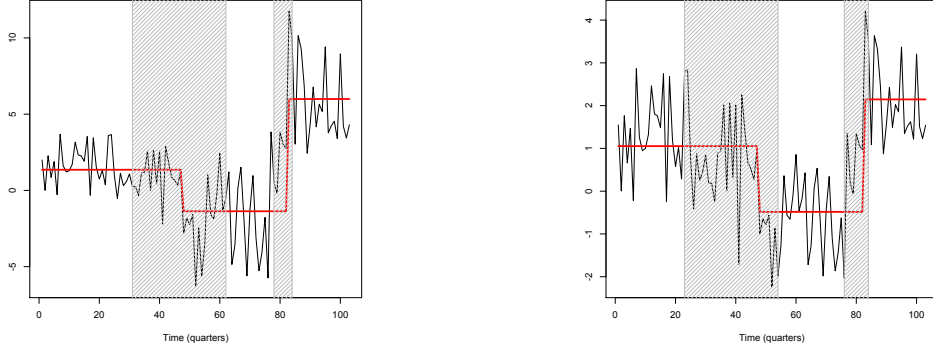


Figure 4: Left plot: time series Y_t ; right plot: time series \tilde{Y}_t ; both with piecewise-constant fits (red) and intervals of significance returned by NSP (shaded grey). See Section 6.1 for a detailed description.

Perron (2003). The dataset is available at <http://qed.econ.queensu.ca/jae/datasets/bai001/>. The dataset Y_t , shown in the left plot of Figure 4, is quarterly and the range is 1961:1–1986:3, so $t = 1, \dots, T = 103$. The arguments outlined in Section J of the appendix justify the applicability of NSP in this context.

We first perform a naive analysis in which we assume our Scenario 1 (piecewise-constant mean) plus i.i.d. $N(0, \sigma^2)$ innovations. This is only so we can obtain a rough segmentation which we can then use to adjust for possible heteroscedasticity of the innovations in the next stage. We estimate σ^2 via $\hat{\sigma}_{MAD}^2$ and run the NSP algorithm (with random interval sampling but having set the random seed to 1, for reproducibility) with the following parameters: $M = 1000$, $\alpha = 0.1$, $\tau_L = \tau_R = 0$. This returns the set \mathcal{S}_0 of two significant intervals: $\mathcal{S}_0 = \{[31, 62], [78, 84]\}$. We estimate the locations of the change-points within these two intervals via CUSUM fits on $Y_{31:62}$ and $Y_{78:84}$; this returns $\hat{\eta}_1 = 47$ and $\hat{\eta}_2 = 82$. The corresponding fit is in the left plot of Figure 4. We then produce an adjusted dataset, in which we divide $Y_{1:47}, Y_{48:82}, Y_{83:103}$ by the respective estimated standard deviations of these sections of the data. The adjusted dataset \tilde{Y}_t is shown in the right plot of Figure 4 and has a visually homoscedastic appearance. NSP run on the adjusted dataset with the same parameters (random seed 1, $M = 1000$, $\alpha = 0.1$, $\tau_L = \tau_R = 0$) produces the significant interval set $\tilde{\mathcal{S}}_0 = \{[23, 54], [76, 84]\}$. CUSUM fits on the corresponding data sections $\tilde{Y}_{23:54}, \tilde{Y}_{76:84}$ produce identical estimated change-point locations $\tilde{\eta}_1 = 47$, $\tilde{\eta}_2 = 82$.

The fit is in the right plot of Figure 4.

We could stop here and agree with Garcia and Perron (1996), who also conclude that there are two change-points in this dataset, with locations within our detected intervals of significance. However, we note that the first interval, $[23, 54]$, is relatively long, so one question is whether it could be covering another change-point to the left of $\tilde{\eta}_1 = 47$. To investigate this, we re-run NSP with the same parameters on $\tilde{Y}_{1:47}$ but find no intervals of significance (not even with the lower thresholds induced by the shorter sample size $T_1 = 47$ rather than the original $T = 103$). Our lack of evidence for a third change-point contrasts with Bai and Perron (2003)'s preference for a model with three change-points.

However, the fact that the first interval of significance $[23, 54]$ is relatively long could also be pointing to model misspecification. If the change of level over the first portion of the data were gradual rather than abrupt, we could naturally expect longer intervals of significance under the misspecified piecewise-constant model. To investigate this further, we now run NSP on \tilde{Y}_t but in Scenario 2, initially in the piecewise-linear model ($q = 1$), which leads to one interval of significance: $\mathcal{S}_1 = \{[73, 99]\}$.

This raises the prospect of modelling the mean of $\tilde{Y}_{1:73}$ as linear. We produce such a fit, in which in addition the mean of $\tilde{Y}_{74:103}$ is modelled as piecewise-constant, with the change-point location $\tilde{\eta}_2 = 79$ found via a CUSUM fit on $\tilde{Y}_{74:103}$. As the middle section of the estimated signal between the two change-points ($\tilde{\eta}_1 = 73$, $\tilde{\eta}_2 = 79$) is relatively short, we also produce an alternative fit in which the mean of $\tilde{Y}_{1:76}$ is modelled as linear, and the mean of $\tilde{Y}_{77:103}$ as constant (the starting point for the constant part was chosen to accommodate the spike at $t = 77$). This is in the right plot of Figure 5 and has a lower BIC value (9.28) than the piecewise-constant fit from the right plot of Figure 4 (10.57). This is because the linear+constant fit uses four parameters, whereas the piecewise-constant fit uses five.

The viability of the linear+constant model for the scaled data \tilde{Y}_t is encouraging because it raises the possibility of a model for the original data Y_t in which the mean of Y_t evolves smoothly in the initial part of the data. We construct a simple example of such a model by fitting the best quadratic on $Y_{1:76}$ (resulting in a strictly decreasing, concave fit), followed by a constant on $Y_{77:104}$. The change-point location, 77, is the same as in the lin-

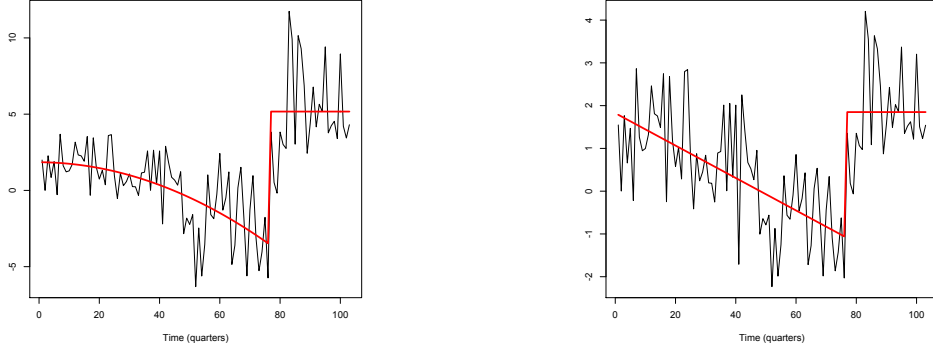


Figure 5: Left plot: Y_t with the quadratic+constant fit; right plot: \tilde{Y}_t with the linear+constant fit. See Section 6.1 for a detailed description.

ear+constant fit for \tilde{Y}_t . The fit is in the left plot of Figure 5. It is interesting to see that the quadratic+constant model for Y_t leads to a lower residual variance than the piecewise-constant model (4.83 to 4.94). Both models use five parameters. We conclude that more general piecewise-polynomial modelling of this dataset can be a viable alternative to the piecewise-constant modelling used in Garcia and Perron (1996) and Bai and Perron (2003). This example shows how NSP, beyond its usual role as an automatic detector of regions of significance, can also serve as a useful tool in achieving improved model selection.

6.2 House prices in London Borough of Newham

We consider the average monthly property price P_t in the London Borough of Newham, for all property types, recorded from January 2010 to November 2020 ($T = 131$) and accessed on 1st February 2021. The data is available on <https://landregistry.data.gov.uk/>. We use the logarithmic scale $Q_t = \log P_t$ and are interested in the stability of the autoregressive model $Q_t = b + aQ_{t-1} + Z_t$. Again, the arguments of Section J of the appendix justify the applicability of NSP here.

NSP, run on a deterministic equispaced interval sampling grid, with $M = 1000$ and $\alpha = 0.1$, with the $\hat{\sigma}_{MOLS}^2$ estimator of the residual variance (see Section D of the appendix) and both with no overlap and with an overlap as defined in formula (12), returns a single interval of significance $[24, 96]$, which corresponds to a likely change-point location between

Table 1: Parameter estimates (standard error in brackets) in the autoregressive model of Section 6.2.

| Parameter | Jan 2010 – Dec 2014 | Jan 2015 – Nov 2020 |
|-----------|---------------------|---------------------|
| b | -0.35 (0.2) | 0.66 (0.23) |
| a | 1.03 (0.02) | 0.95 (0.02) |

December 2011 and December 2017. Assuming a possible change-point in the middle of this interval, i.e. in December 2014, we run two autoregressions (up to December 2014 and from January 2015 onwards) and compare the coefficients. Table 1 shows the estimated regression coefficients (with their standard errors) over the two sections.

It appears that both the intercept and the autoregressive parameter change significantly at the change-point. In particular, the change in the autoregressive parameter from 1.03 (standard error 0.02) to 0.95 (0.02) suggest a shift from a unit-root process to a stationary one. This agrees with a visual assessment of the character of the process in the right plot of Figure 3, where it appears that the process is more ‘trending’ before the change-point than it is after, where it exhibits a conceivably stationary behaviour, particularly from the middle of 2016 or so. Indeed, the average monthly change in Q_t over the time period Jan 2010 – Dec 2014 is 0.0061, larger than the corresponding average change of 0.0052 over Jan 2015 – Nov 2020.

Appendix

A Additional literature review

We first comment in more detail on the UD max and WD max tests of Bai and Perron (1998) and Bai and Perron (2003) and their relationship to NSP. Bai and Perron (2003) write:

A useful strategy is to first look at the UD max or WD max tests to see if at least one break is present. If these indicate the presence of at least one break, then the number of breaks can be decided based upon a sequential examination of the sup $F(l+1|l)$ statistics constructed using global minimizers for the break

dates (i.e. ignore the test $F(1|0)$ and select m such that the tests $\sup F(l + 1|l)$ are insignificant for $l \geq m$). This method leads to the best results and is recommended for empirical applications.

For the purpose of this discussion, we label the process above the ‘Improved Sequential Procedure’ (ISP). Bai and Perron (2003) do not formulate or prove the inferential properties of the m selected by ISP. For a procedure that selects the number of change-points, the control of global significance would have to mean, in particular, a guarantee that the true number of change-points is at least as high as the estimated number, with at least $1 - \alpha$ probability. NSP provides such a statement as a simple corollary of Theorem 2.1, but ISP is a complex sequential process put together from separate, non-independent, conditionally applied tests, and the exact guarantees for the resulting output (m) have not been shown.

The next difference is that the UD max and WD max tests require the provision of the maximum number of change-points, but NSP does not require this, thereby eliminating the risk of providing too low a maximum by the user.

Furthermore, the ISP test only concerns the number of change-points, but not their locations: inference for locations in Bai and Perron (1998) and Bai and Perron (2003) is carried out later, *conditionally* on the number of change-points and on their estimated locations. Not only that, but also the obtained conditional confidence intervals are asymptotic in nature and are only valid for large sample sizes (unknown to the user). By contrast, NSP provides a single, clear, joint, finite-sample guarantee for the number of change-points and for their locations: it flags up disjoint regions in the data, each of which must contain at least one change-point with a global probability specified by the user. The NSP intervals of significance serve as “unconditional” confidence intervals (in contrast to the conditional CIs of Bai and Perron (1998) and Bai and Perron (2003), whose conditionality on the number of estimated change-points and the estimated locations means that the user cannot be sure whether they contain change-points with a certain probability). The NSP guarantees are valid for any, even small, sample sizes.

Next, we discuss in more detail the most important high-level differences between NSP and the approaches of Fang et al. (2020) and Fang and Siegmund (2020).

- (a) While Fang et al. (2020) and Fang and Siegmund (2020) perform change-point location estimation as well as inference, NSP works on the principle of “inference without location estimation”. This is a key property of NSP, which enables it to use an all-purpose multiscale test, whose distribution under the null is stochastically bounded by the scan statistic of the corresponding true residuals Z_t , and is therefore independent of the scenario and of the design matrix X used. This means that NSP is ready for use with any user-provided design matrix X , and this will require no new calculations or coding, and will yield correct coverage probabilities. This is in contrast to the approach taken in Fang et al. (2020) and Fang and Siegmund (2020), in which, because of their focus on location estimation, each new scenario not already covered would involve new and fairly complicated approximations of the null distribution. (We note that outside the change-point context, the method for constructing confidence intervals for groups of variables in sparse high dimensional regression by Meinshausen (2015) shares with NSP the attractive property of providing valid error control without assumptions on the design matrix.)
- (b) While in Fang et al. (2020) and Fang and Siegmund (2020), the user needs to be able to specify the significant signal shapes to look for, NSP searches for any deviations from local model linearity with respect to specific regressors.
- (c) Out of our scenarios, Fang et al. (2020) and Fang and Siegmund (2020) provide results under our Scenario 1 and Scenario 2 with linearity and continuity. Their results do not cover our Scenario 3 (linear regression with arbitrary X) or Scenario 2 with linearity but not necessarily continuity, or Scenario 2 with higher-than-linear polynomials.
- (d) Thanks to its double use of the multiresolution sup-norm (in the local linear fit, and then in the test of this fit), NSP is able to handle regression with autoregression practically in the same way as without, in a stable manner and on arbitrarily short intervals, and does not suffer from having to estimate the unknown (nuisance) AR coefficients accurately. This is of importance, as change-point analysis under serial dependence in the data is a well-known difficult problem, and NSP offers a new approach to it, thanks to this feature.

B Discussion of the NSP algorithm

We now comment on a few generic aspects of the NSP algorithm.

Length check for $[s, e]$ in line 2 Consider an interval $[s, e]$ with $e - s < p$. If it is known that the matrix $X_{s:e,\cdot}$ is of rank $e - s + 1$ (as is the case, for example, in Scenario 2, for all such s, e) then it is safe to disregard $[s, e]$, as the response $Y_{s:e}$ can then be explained exactly as a linear combination of the columns of $X_{s:e,\cdot}$, so it is impossible to assess any deviations from linearity of $Y_{s:e}$ with respect to $X_{s:e,\cdot}$. Therefore, if this rank condition holds, the check in line 2 of NSP can be replaced with $e - s < p$, which (together with the corresponding modifications in lines 5–10) will reduce the computational effort if $p > 1$. Having $p = p(T)$ growing with T is possible in NSP, but by the above discussion, we must have $p(T) + 1 \leq T$ or otherwise no regions of significance will be found.

Sub-interval sampling Sub-interval sampling in lines 5–10 of the NSP algorithm is done to reduce the computational effort. In the change-point detection literature (without inference considerations), Wild Binary Segmentation (WBS, Fryzlewicz, 2014) uses a random interval sampling mechanism in which all or almost all intervals are sampled at the start of the procedure, i.e. with all or most intervals not being sampled recursively. The same style of interval sampling is used in the Narrowest-Over-Threshold change-point detection (note: not change-point inference) algorithm (Baranowski et al., 2019) and is mentioned in passing in Fang et al. (2020). Instead, NSP uses a different, recursive interval sampling mechanism, introduced in the change-point detection (not inference) context in Wild Binary Segmentation 2 (WBS2, Fryzlewicz, 2020). In NSP (lines 5–10), intervals are sampled separately in each recursive call of the NSP routine. As argued in Fryzlewicz (2020), this enables more thorough exploration of the domain $\{1, \dots, T\}$ and hence better feature discovery than the non-recursive sampling style. We note that NSP can equally use random or deterministic interval selection mechanisms; a specific example of a deterministic interval sampling scheme in a change-point detection context can be found in Kovács et al. (2022).

Relationship to NOT The Narrowest-Over-Threshold (NOT) algorithm of Baranowski et al. (2019) is a change-point detection procedure (valid in Scenarios 1 and 2) and comes with no inference considerations. The common feature shared by NOT and NSP is that in their respective aims (change-point detection for NOT; locating regions of global significance for NSP) they iteratively focus on the narrowest intervals on which a certain test (a change-point locator for NOT; a multiscale scan statistic on multiresolution sup-norm fit residuals for NSP) exceeds a threshold, but this is where similarities end: apart from this common feature, the objectives, scopes and *modi operandi* of both methods are different.

Focus on the smallest significant regions Some authors in the inference literature also identify the shortest intervals (or smallest regions) of significance in data. For example, Dümbgen and Walther (2008) plot minimal intervals on which a density function significantly decreases or increases. Walther (2010) plots minimal significant rectangles on which the probability of success is higher than a baseline, in a two-dimensional spatial model. Fang et al. (2020) mention the possibility of using the interval sampling scheme from Fryzlewicz (2014) to focus on the shortest intervals in their CUSUM-based determination of regions of significance in Scenario 1. In addition to NSP’s new definition of significance involving the multiresolution sup-norm fit (whose benefits are explained in Section 2.2), NSP is also different from these approaches in that its pursuit of the shortest significant intervals is at its algorithmic core and is its main objective. To achieve it, NSP uses a number of solutions which, to the best of our knowledge, either are new or have not been considered in this context before. These include the two-stage search for the shortest significant subinterval (NSP routine, line 19) and the recursive sampling (lines 5–10, proposed previously but in a non-inferential context by Fryzlewicz (2020)).

Lack of penalisation for fine scales. Instead of using multiresolution sup-norms (multiscale scan statistics), some authors, including Walther (2010) and Frick et al. (2014), use alternative definitions which penalise fine scales (i.e. short intervals) in order to enhance detection power at coarser scales. We do not pursue this route, as NSP aims to discover significant intervals that are as short as possible, and hence we are interested in retaining good

detection power at fine scales. However, some natural penalisation of fine scales necessarily occurs in the self-normalised case; see Section 3.1.

Upper bounds for p -values on non-detection intervals. By calculating the quantity $D_{[s,e]}$ on each data section $[s,e]$ delimited by the detected intervals of significance, an upper bound on the p -value for the existence of a change-point in $[s,e]$ can be obtained as $P(\|Z\|_{\mathcal{I}^a} > D_{[s,e]})$. If the interval $[s,e]$ were considered by NSP before (as would be the case e.g. if $\tau_L = \tau_R = 0$ and the deterministic sampling grid were used), from the non-detection on $[s,e]$, we would necessarily have $P(\|Z\|_{\mathcal{I}^a} > D_{[s,e]}) \geq \alpha$.

C Proofs of results of Section 2

Proof of Proposition 2.1. As $[s,e]$ does not contain a change-point, there is a β^* such that $Y_{s:e} = X_{s:e} \cdot \beta^* + Z_{s:e}$. Therefore, $D_{[s,e]} = \min_{\beta} \|Y_{s:e} - X_{s:e} \cdot \beta\|_{\mathcal{I}_{[s,e]}^d} \leq \|Y_{s:e} - X_{s:e} \cdot \beta^*\|_{\mathcal{I}_{[s,e]}^d} = \|Z_{s:e}\|_{\mathcal{I}_{[s,e]}^d}$, which completes the proof. \square

Proof of Theorem 2.1. The second inequality is implied by (4). We now prove the first inequality. On the set $\|Z\|_{\mathcal{I}^d} \leq \lambda_{\alpha}$, each interval S_i must contain a change-point as if it did not, then by Proposition 2.1, we would have to have

$$D_{S_i} \leq \|Z\|_{\mathcal{I}^d} \leq \lambda_{\alpha}. \quad (13)$$

However, the fact that S_i was returned by NSP means, by line 14 of the NSP algorithm, that $D_{S_i} > \lambda_{\alpha}$, which contradicts (13). This completes the proof. \square

D Estimated σ^2 , and other light-tailed distributions

We first show under what condition Theorem 2.2 remains valid with an estimated variance σ^2 , and give an estimator of σ^2 that satisfies this condition for certain matrices X and parameter vectors $\beta^{(j)}$. Similar considerations are possible for the light-tailed distributions from the latter part of this section, but we omit them here. With $\{Z_t\}_{t=1}^T \sim N(0, \sigma^2)$ rather

than $N(0, 1)$, the statement of Theorem 2.2 trivially modifies to

$\lim_{T \rightarrow \infty} P(\max_{1 \leq s \leq e \leq T} U_{s,e}(Z) \leq \sigma(a_T + b_T \gamma)) = \exp(-e^{-\gamma})$. From the form of the limiting distribution, it is clear that the theorem remains valid if $\gamma_T \xrightarrow{T \rightarrow \infty} \gamma$ is used in place of γ , yielding

$$\lim_{T \rightarrow \infty} P\left(\max_{1 \leq s \leq e \leq T} U_{s,e}(Z) \leq \sigma(a_T + b_T \gamma_T)\right) = \exp(-e^{-\gamma}). \quad (14)$$

With σ estimated via a generic estimator $\hat{\sigma}$, we ask under what circumstances

$$\lim_{T \rightarrow \infty} P\left(\max_{1 \leq s \leq e \leq T} U_{s,e}(Z) \leq \hat{\sigma}(a_T + b_T \gamma)\right) = \exp(-e^{-\gamma}). \quad (15)$$

In light of (14), it is enough to solve for γ_T in $\sigma(a_T + b_T \gamma_T) = \hat{\sigma}(a_T + b_T \gamma)$, yielding $\gamma_T = \frac{a_T}{b_T} \left(\frac{\hat{\sigma}}{\sigma} - 1\right) + \frac{\hat{\sigma}}{\sigma} \gamma$. In view of the form of a_T and b_T defined in Theorem 2.2, we have $\gamma_T \xrightarrow{T \rightarrow \infty} \gamma$ on a set large enough for (15) to hold if

$$\left|\frac{\hat{\sigma}}{\sigma} - 1\right| = o_P(\log^{-1} T), \quad \text{or equivalently} \quad \left|\frac{\hat{\sigma}^2}{\sigma^2} - 1\right| = o_P(\log^{-1} T). \quad (16)$$

After Rice (1984) and Dümbgen and Spokoiny (2001), define $\hat{\sigma}_R^2 = \frac{1}{2(T-1)} \sum_{t=1}^{T-1} (Y_{t+1} - Y_t)^2$. Define the signal in model (2) by $f_t = X_{t,\cdot} \beta^{(j)}$ for $t = \eta_j + 1, \dots, \eta_{j+1}$, for $j = 0, \dots, N$. The total variation of a vector $\{f_t\}_{t=1}^T$ is defined by $TV(f) = \sum_{t=1}^{T-1} |f_{t+1} - f_t|$. As in Dümbgen and Spokoiny (2001), we have $\mathbb{E}\{(\hat{\sigma}_R^2/\sigma^2 - 1)^2\} = O(T^{-1}\{1 + TV^2(f)\})$, from which (16) follows, by Markov inequality, if

$$TV(f) = o(T^{1/2} \log^{-1} T). \quad (17)$$

By way of a simple example, in Scenario 1, $TV(f) = \sum_{j=1}^N |f_{\eta_j} - f_{\eta_{j+1}}|$, and therefore (17) is satisfied if the sum of jump magnitudes in f is $o(T^{1/2} \log^{-1} T)$. Note that if f is bounded with a number of change-points that is finite in T , then $TV(f) = \text{const}(T)$. Similar arguments apply in Scenario 2, and in Scenario 3 for some matrices X .

Without formal theoretical justifications, we also mention two further estimators of σ^2 (or σ) which we use in our numerical work. In Scenarios 1 and 2, we use $\hat{\sigma}_{MAD}$, the Median Absolute Deviation (MAD) estimator as implemented in the R routine `mad`, computed on the

sequence $\{2^{-1/2}(Y_{t+1} - Y_t)\}_{t=1}^{T-1}$. Empirically, $\hat{\sigma}_{MAD}$ is more robust than $\hat{\sigma}_R$ to the presence of change-points in f_t , but is also more sensitive to departures from the Gaussianity of Z_t . In Scenario 3, in settings outside Scenarios 1 and 2, we use the following estimator. In model (2), we estimate σ via least squares, on a rolling window basis, using the window of size $w = \min\{T, \max([T^{1/2}], 20)\}$, to obtain the sequence of estimators $\hat{\sigma}_1, \dots, \hat{\sigma}_{T-w+1}$. We take $\hat{\sigma}_{MOLS} = \text{median}(\hat{\sigma}_1, \dots, \hat{\sigma}_{T-w+1})$, where MOLS stands for ‘Median of OLS estimators’. The hope is that most of the local estimators $\hat{\sigma}_1, \dots, \hat{\sigma}_{T-w+1}$ are computed on change-point-free sections of the data, and therefore the median of these local estimators should serve as an accurate estimator of the true σ . Empirically, $\hat{\sigma}_{MOLS}$ is a useful alternative to $\hat{\sigma}_R$ in settings in which condition (17) is not satisfied.

Kabluchko and Wang (2014) provide a result similar to Theorem 2.2 for distributions of Z dominated by the Gaussian in a sense specified below. These include, after scaling so that $\mathbb{E}(Z) = 0$ and $\text{Var}(Z) = 1$, the symmetric Bernoulli, symmetric binomial and uniform distributions, amongst others. We now briefly summarise it. Consider the cumulant-generating function of Z defined by $\varphi(u) = \log \mathbb{E}(e^{uZ})$ and assume that for some $\sigma_0 > 0$, we have $\varphi(u) < \infty$ for all $u \geq -\sigma_0$. Assume further that for all $\varepsilon > 0$, $\sup_{u \geq \varepsilon} \varphi(u)/(u^2/2) < 1$. Finally, assume

$$\varphi(u) = \frac{u^2}{2} - \kappa u^d + o(u^d), \quad u \downarrow 0,$$

for some $d \in \{3, 4, \dots\}$ and $\kappa > 0$. Typical values of d for non-symmetric and symmetric distributions, respectively, are 3 and 4. Under these assumptions, we have

$$\lim_{T \rightarrow \infty} P \left(\frac{1}{2} \left\{ \max_{1 \leq s \leq e \leq T} U_{s,e}(Z) \right\}^2 \leq \log \left\{ T \log^{\frac{d-6}{2(d-2)}} T \right\} + \gamma \right) = \exp(-\Lambda_{d,\kappa} e^{-\gamma}),$$

for all $\gamma \in \mathbb{R}$, where $\Lambda_{d,\kappa} = \pi^{-1/2} \Gamma(d/(d-2)) (2\kappa)^{2/(d-2)}$. After simple algebraic manipulations, this result permits a selection of λ_α for use in Theorem 2.1, similarly to Section 2.3.

E Importance of two-stage search for shortest interval of significance

We next illustrate the importance of the two-stage search for the shortest interval of significance, whose stage two is performed in line 19 of the NSP algorithm via the call

$$[\tilde{s}, \tilde{e}] := \text{SHORTESTSIGNIFICANTSUBINTERVAL}(s_{m_0}, e_{m_0}, Y, X, M, \lambda_\alpha).$$

Consider the `blocks` signal but with the much smaller noise standard deviation $\sigma = 1$. A realisation Y_t is shown in the left plot of Figure 6. All $N = 11$ change-points are visually obvious and hence we would expect NSP to return 11 intervals $[\tilde{s}_i, \tilde{e}_i]$, exactly covering the true change-points, for which we would have $\tilde{e}_i - \tilde{s}_i = 1$ for most if not all i . As shown in the middle plot of Figure 6, the NSP procedure with no overlap and with the same parameters as in Section 5.1.1 returns 11 intervals of significance with $\tilde{e}_i - \tilde{s}_i = 1$ for $i = 1, \dots, 10$ and $\tilde{e}_{11} - \tilde{s}_{11} = 2$. The 11 intervals of significance cover the true change-points.

However, consider now an alternative version of NSP, labelled NSP(1), which only performs a one-stage search for the shortest interval of significance. NSP(1) proceeds by replacing line 19 of the NSP algorithm by

$$[\tilde{s}, \tilde{e}] := [s_{m_0}, e_{m_0}].$$

In other words, $[s_{m_0}, e_{m_0}]$ is not searched for its shortest sub-interval of significance, but is added to \mathcal{S} as it is. The output of NSP(1) on Y_t is shown in the right plot of Figure 6. The intervals of significance returned by NSP(1) are unreasonably long from the statistical point of view, with $\tilde{e}_i - \tilde{s}_i$ varying from 2 to 45. However, this has a clear explanation from the point of view of the algorithmic construction of NSP(1). For example, in the first recursive stage, in which $[s, e] = [1, T]$, the spacing of the (approximately) equispaced grid from which the candidate intervals $[s_m, e_m]$ are drawn varies between 45 and 46. Therefore, it is unsurprising that the first detection performed by NSP(1) is such that $\tilde{e}_i - \tilde{s}_i = 45$.

This issue would not arise in NSP, as NSP would then search this detection interval for its

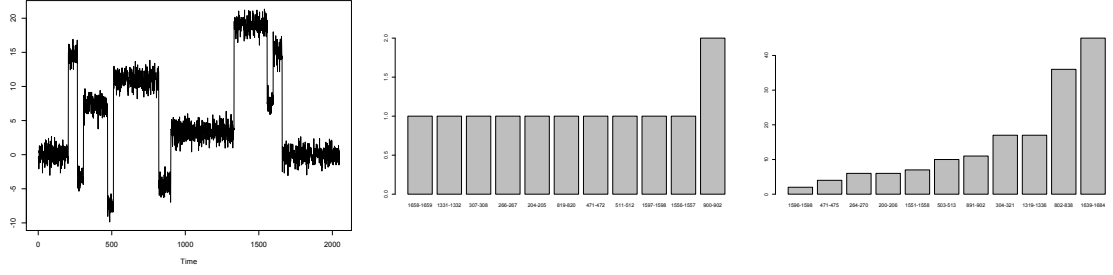


Figure 6: Left: realisation Y_t of noisy **blocks** with $\sigma = 1$. Middle: prominence plot of NSP-detected intervals. Right: the same for NSP(1). See Section E for more details.

shortest significant sub-interval. From the output of the NSP procedure, we can see that this second-stage search drastically reduced the length of this detection interval, which is unsurprising given how obvious the change-points are in this example. This illustrates the importance of the two-stage search in NSP.

For very long signals, it is conceivable that an analogous three-stage search may be a better option, possibly combined with a reduction in M to enhance the speed of the procedure.

F Self-normalised NSP – further discussion

We now outline the construction of $\hat{Z}^{(k)}$ for $k = 1, 2, 3$ so that (8) is guaranteed, and propose a suitable estimator of V_T^2 for use in (8).

$k = 1$. Let $(\hat{Z}_{i+1}^{(1)}, \dots, \hat{Z}_j^{(1)})$ be the ordinary least-squares residuals from regressing $Y_{(i+1):j}$ on $X_{(i+1):j,\cdot}$, where $j - i > p$. As $[s, e]$ contains no change-point, we have $(\hat{Z}_{i+1}^{(1)})^2 + \dots + (\hat{Z}_j^{(1)})^2 \leq Z_{i+1}^2 + \dots + Z_j^2$ and hence $\log^{1/2+\epsilon}\{cV_T^2/((\hat{Z}_{i+1}^{(1)})^2 + \dots + (\hat{Z}_j^{(1)})^2)\} \geq \log^{1/2+\epsilon}\{cV_T^2/(Z_{i+1}^2 + \dots + Z_j^2)\}$.

$k = 2$. We use

$$(\hat{Z}_{i+1}^{(2)}, \dots, \hat{Z}_j^{(2)}) = (1 + \epsilon)(\hat{Z}_{i+1}^{(1)}, \dots, \hat{Z}_j^{(1)}), \quad (18)$$

which guarantees $(\hat{Z}_{i+1}^{(2)})^2 + \dots + (\hat{Z}_j^{(2)})^2 \geq Z_{i+1}^2 + \dots + Z_j^2$ for ϵ and $j - i$ suitably large, for a range of distributions of Z_t and design matrices X . We now briefly sketch the argument justifying this for Scenario 1; similar considerations are possible in Scenario 2

but are notationally much more involved and we omit them here. The argument relies again on self-normalisation. From standard least-squares theory (in any Scenario), we have

$$(\hat{Z}_{(i+1):j}^{(1)})^\top \hat{Z}_{(i+1):j}^{(1)} = Z_{(i+1):j}^\top Z_{(i+1):j} - Z_{(i+1):j}^\top X_{(i+1):j,\cdot} (X_{(i+1):j,\cdot}^\top X_{(i+1):j,\cdot})^{-1} X_{(i+1):j,\cdot}^\top Z_{(i+1):j}.$$

In Scenario 1, $(X_{(i+1):j,\cdot}^\top X_{(i+1):j,\cdot})^{-1} = (j-i)^{-1}$, and hence

$Z_{(i+1):j}^\top X_{(i+1):j,\cdot} (X_{(i+1):j,\cdot}^\top X_{(i+1):j,\cdot})^{-1} X_{(i+1):j,\cdot}^\top Z_{(i+1):j} = U_{i+1,j}(Z)^2$. From the above, we obtain

$$\begin{aligned} (\hat{Z}_{(i+1):j}^{(1)})^\top \hat{Z}_{(i+1):j}^{(1)} &= Z_{(i+1):j}^\top Z_{(i+1):j} \left(1 - \frac{U_{i+1,j}(Z)^2}{Z_{(i+1):j}^\top Z_{(i+1):j}} \right) \\ &= Z_{(i+1):j}^\top Z_{(i+1):j} \left(1 - \frac{1}{j-i} \log^{1+2\epsilon} \{cV_T^2 / (Z_{i+1}^2 + \dots + Z_j^2)\} \right) \\ &\times I_{\rho_{1/2,1/2+\epsilon,c}}^2(\zeta_T^{\text{se}}, V_i^2/V_T^2, V_j^2/V_T^2). \end{aligned} \quad (19)$$

In light of the distributional result (7), the relationship between the statistic $I_{\rho_{1/2,1/2+\epsilon,c}}(W, u, v)$ and Račkauskas and Suquet (2004)'s statistic $\text{UI}(\rho_{1/2,1/2+\epsilon,c})$, as well as their Remark 5, we are able to bound $\sup_{0 \leq i < j \leq T} I_{\rho_{1/2,1/2+\epsilon,c}}^2(\zeta_T^{\text{se}}, V_i^2/V_T^2, V_j^2/V_T^2)$ by a term of order $O(\log T)$ on a set of probability $1 - O(T^{-1})$. Making the mild assumption that $\sup_{0 \leq i < j \leq T} \log^{1+2\epsilon} \{cV_T^2 / (Z_{i+1}^2 + \dots + Z_j^2)\} \asymp l_T = o_P(T \log^{-1} T)$ and continuing from (19), we obtain $(\hat{Z}_{(i+1):j}^{(1)})^\top \hat{Z}_{(i+1):j}^{(1)} \geq Z_{(i+1):j}^\top Z_{(i+1):j} (1 - C(j-i)^{-1} l_T \log T)$ for a certain constant $C > 0$, which can be bounded from below by $Z_{(i+1):j}^\top Z_{(i+1):j} (1+\epsilon)^{-2}$, uniformly over those i, j for which $(j-i)^{-1} l_T \log T \rightarrow 0$. This justifies (18) and completes the argument.

$k = 3$. Having obtained $\hat{Z}_{(i+1):j}^{(1)}$ and $\hat{Z}_{(i+1):j}^{(2)}$ as above, the problem of obtaining $\hat{Z}_{s:e}^{(3)}$ to guarantee

$$\begin{aligned} &\sup_{s-1 \leq i < j \leq e} \frac{|\hat{Z}_{i+1}^{(3)} + \dots + \hat{Z}_j^{(3)}|}{\sqrt{(\hat{Z}_{i+1}^{(2)})^2 + \dots + (\hat{Z}_j^{(2)})^2} \log^{1/2+\epsilon} \{cV_T^2 / ((\hat{Z}_{i+1}^{(1)})^2 + \dots + (\hat{Z}_j^{(1)})^2)\}} \\ &\leq \sup_{s-1 \leq i < j \leq e} \frac{|Z_{i+1} + \dots + Z_j|}{\sqrt{(\hat{Z}_{i+1}^{(2)})^2 + \dots + (\hat{Z}_j^{(2)})^2} \log^{1/2+\epsilon} \{cV_T^2 / ((\hat{Z}_{i+1}^{(1)})^2 + \dots + (\hat{Z}_j^{(1)})^2)\}}, \end{aligned} \quad (20)$$

which in turn guarantees the bound (8), is practically equivalent to the multiresolution norm minimisation solved in Step 1 of Section 2.2 except it now uses a weighted version of the norm $\|\cdot\|_{\mathcal{I}_{[s,e]}^a}$, where the weights are given in the denominator of (20). This weighted

problem is solved via linear programming just as easily as Step 1 of Section 2.2, the only difference being that the relevant constraints are multiplied by the corresponding weights.

We now discuss further practicalities of the self-normalisation. In the exposition earlier, we use all intervals $[i + 1, j] \subseteq [s, e]$, i.e. the set $\mathcal{I}_{[s,e]}^a$. In practice, for computational reasons, we compute the supremum on the LHS of (8) over the dyadic set $\mathcal{I}_{[s,e]}^d$, which does not alter the validity of the bound. Our empirical experience is that the statistic on the LHS of (8) is fairly robust to the choice of V_T^2 , as the latter only enters through the (close to) square-root logarithmic term in the denominator. In addition, over-estimation of V_T^2 for use on the LHS of (8) is permitted as it only strengthens the bound in (8). For these reasons, we do not dwell on the accurate estimation of V_T^2 here, but use the rough estimate $\hat{V}_T^2 = \frac{T}{T-w+1} \sum_{t=1}^{T-w+1} \hat{\sigma}_t^2$, where the $\hat{\sigma}_t$'s are the constituents of the $\hat{\sigma}_{MOLS}$ estimator from Section D. As clarified earlier, the use of (18) requires that small values of $j - i$ do not enter in the computation of the supremum on the LHS of (8). In practice, however, we use all $[i + 1, j] \in \mathcal{I}_{[s,e]}^d$. This is because the function $I_{\rho_{1/2,1/2+\epsilon,c}}(\zeta_T^{\text{se}}, V_i^2/V_T^2, V_j^2/V_T^2)$ naturally penalises small scales (i.e. short intervals $[i + 1, j]$) through the use of the logarithmic term in the denominator. Therefore, in practice, short intervals $[i + 1, j]$ do not tend to achieve the supremum on the LHS of (8) and as a result, we have found further exclusion of such short intervals unnecessary. Finally, we have experimented with ϵ in the range $[0.03, 0.1]$ and found little difference in practical performance. Our code uses $\epsilon = 0.03$ as a default.

G NSP with autoregression

We use the piecewise-constant signal of length $T = 1000$ from the first simulation setting in Dette et al. (2020), contaminated with Gaussian AR(1) noise with coefficient 0.9 and standard deviation $(1 - 0.9^2)^{-1/2}/5$. A sample path, together with the true change-point locations, is shown in Figure 7.

We run the AR version of the NSP algorithm (as outlined in Section 3.2), with the following parameters: a deterministic equispaced interval sampling grid, $M = 100$, $\alpha = 0.1$, no overlap, $\hat{\sigma}_{MOLS}^2$ estimator of the residual variance. The resulting intervals are shown in

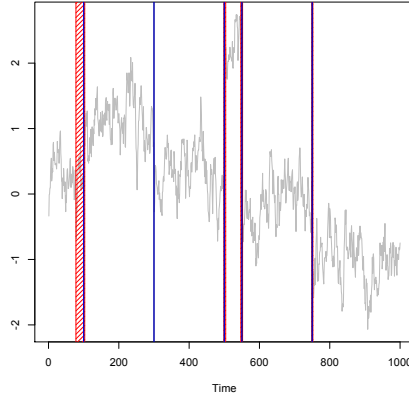


Figure 7: Piecewise-constant signal from Dette et al. (2020) with Gaussian AR(1) noise with coefficient 0.9 and standard deviation $(1 - 0.9^2)^{-1/2}/5$ (light grey), NSP intervals of significance (shaded red), true change-points (blue); see Section G for details.

Table 2: Percentage of sample paths with the given numbers of NSP-detected intervals in the autoregressive example of Section G.

| | | | | |
|----------------------------------|----|----|----|----|
| no. of intervals of significance | 2 | 3 | 4 | 5 |
| percentage of sample paths | 11 | 32 | 42 | 15 |

Figure 7; NSP intervals cover four out of the five true change-points, and there are no spurious intervals.

We simulate from this model 100 times and obtain the following results. In 100% of the sample paths, each NSP interval of significance covers one true change-point (which fulfils the promise of Theorem 2.1). The distribution of the detected numbers of intervals is as in Table 2; we recall that NSP, with a fixed significance level, does not promise to detect the number of intervals equal to the number of true change-points in the underlying process.

H Detection consistency and lengths of NSP intervals – proofs and discussion

Proof of Theorem 4.1. Assume initially that f_t has a single change-point η_1 . As NSP considers all intervals by the assumption of the theorem, it will certainly consider intervals symmetric about the true change-point, i.e. $[\eta_1 - d + 1, \eta_1 + d]$, for all appropriate d . In

Scenario 1, there is an explicit formula for the deviation measure $D_{[s,e]}$ on any interval $[s, e]$, given by

$$D_{[s,e]} = \max_{\tau \in \{1, \dots, e-s+1\}} \frac{1}{2\sqrt{\tau}} \left(\max_{s_1 \in \{s, \dots, e+1-\tau\}} \sum_{t=s_1}^{s_1+\tau-1} Y_t - \min_{s_1 \in \{s, \dots, e+1-\tau\}} \sum_{t=s_1}^{s_1+\tau-1} Y_t \right). \quad (21)$$

Without loss of generality, assume $f_{\eta_1} > f_{\eta_1+1}$. Representation (21) implies

$$\begin{aligned} D_{[\eta_1-d+1, \eta_1+d]} &\geq \frac{1}{2\sqrt{d}} \left(\max_{s_1 \in \{\eta_1-d+1, \dots, \eta_1+1\}} \sum_{t=s_1}^{s_1+d-1} Y_t - \min_{s_1 \in \{\eta_1-d+1, \dots, \eta_1+1\}} \sum_{t=s_1}^{s_1+d-1} Y_t \right) \\ &\geq \frac{1}{2\sqrt{d}} \left(\sum_{t=\eta_1-d+1}^{\eta_1} Y_t - \sum_{t=\eta_1+1}^{\eta_1+d} Y_t \right) \\ &\geq \frac{1}{2} |f_{\eta_1+1} - f_{\eta_1}| \sqrt{d} - \|Z\|_{\mathcal{I}^a}. \end{aligned} \quad (22)$$

On the set $\|Z\|_{\mathcal{I}^a} \leq \lambda_\alpha$, (22) is further bounded from below by $\frac{1}{2} |f_{\eta_1+1} - f_{\eta_1}| \sqrt{d} - \lambda_\alpha$. From the definition of the NSP algorithm, detection on $[s, e]$ is triggered by the event $D_{[s,e]} > \lambda_\alpha$, so detection on $[\eta_1 - d + 1, \eta_1 + d]$ is triggered if (note: not “only if” as we are using lower bounds here) $\frac{1}{2} |f_{\eta_1+1} - f_{\eta_1}| \sqrt{d} - \lambda_\alpha > \lambda_\alpha$, or

$$|f_{\eta_1+1} - f_{\eta_1}| \sqrt{d} > 4\lambda_\alpha. \quad (23)$$

As NSP looks for shortest intervals of detection, the NSP interval of significance around η_1 will definitely be no longer than $2d = |[\eta_1 - d + 1, \eta_1 + d]|$. However, from (23), it is sufficient for detection to be triggered if $d > \frac{16\lambda_\alpha^2}{|f_{\eta_1+1} - f_{\eta_1}|^2}$. This shows that the maximum length of an NSP interval of significance will not exceed $2\bar{d}$, where $\bar{d} = \left\lceil \frac{16\lambda_\alpha^2}{|f_{\eta_1+1} - f_{\eta_1}|^2} \right\rceil + 1$. We now turn our attention to the multiple change-point case. For each change-point η_j , define its corresponding \bar{d}_j as in formula (10). Recall we are on the set $\|Z\|_{\mathcal{I}^a} \leq \lambda_\alpha$. Note first that even though the NSP interval of significance around η_j is guaranteed to be of length at most $2\bar{d}_j$, it will not necessarily be a subinterval of $[\eta_j - \bar{d}_j + 1, \eta_j + \bar{d}_j]$ (as NSP simply looks for the shortest intervals of significance and interval symmetry around the true change-point is not promoted). Therefore, in order that an interval detection around η_j does not interfere with detections around η_{j-1} and η_{j+1} , the distances $\eta_j - \eta_{j-1}$ and $\eta_{j+1} - \eta_{j-1}$ must be

suitably long, but this is guaranteed by Assumption 4.1. This completes the proof. \square

As an aside, note in addition that in the Gaussian case $Z_t \sim N(0, 1)$, Theorem 2.2 implies $\lambda_\alpha = O(\log^{1/2} T)$; in fact for $\alpha = 0.05$, we have $\lambda_\alpha \leq 1.33\sqrt{2\log T}$ for $T \geq 100$, for $\alpha = 0.1$, we have $\lambda_\alpha \leq 1.25\sqrt{2\log T}$ over the same range of T .

Proof of Corollary 4.1. From Lemma 1 in Yao (1988), we have

$$P(\|Z\|_{\mathcal{I}^a} \leq \sigma(1 + \Delta)\sqrt{2\log T}) \rightarrow 1$$

as $T \rightarrow \infty$. This combined with the statement of Theorem 4.1 proves the result. \square

Proof of Theorem 4.2. Assume initially that f_t has a single change-point η_1 . In the same way in which the NSP procedure is “blind” to constant shifts in the data in Scenario 1, it is also invariant to the addition of linear trends in the piecewise-linear Scenario 2. Assume, therefore, that we have added a linear trend to Y_t in such a way that the true signal is symmetric around the true change-point η_1 . The case that will lead to the longest interval is one in which the change-point leads to a trapezoid shape of the true signal (as in, for example, 1, 2, 3, 3, 2, 1) rather than one with a single peak or trough (e.g. 1, 2, 3, 2, 1). Therefore we assume the former case as the “worst case” (whether this is or is not assumed will only lead to $O(1)$ differences in the length of the NSP intervals, so is irrelevant from the point of view of rates). Note that for such a trapezoid signal, the location of η_1 is unambiguous (in the cartoon example above, it must be at the first 3). For such a transformed signal (a transformation which does not change the output of the NSP algorithm), consider intervals symmetric around the true change-point, i.e. $[\eta_1 - d + 1, \eta_1 + d]$, which will be considered by this version of NSP as it considers all intervals. We have

$$D_{[\eta_1 - d + 1, \eta_1 + d]} = \min_{\tilde{f}_{(\eta_1 - d + 1):(\eta_1 + d)}} \|Y_{(\eta_1 - d + 1):(\eta_1 + d)} - \tilde{f}_{(\eta_1 - d + 1):(\eta_1 + d)}\|_{\mathcal{I}_{[\eta_1 - d + 1, \eta_1 + d]}^a}, \quad (24)$$

where the minimum is taken with respect to all linear fits on $[\eta_1 - d + 1, \eta_1 + d]$. Consider a single scale τ . Observing that taking moving partial sums does not change the linearity of

\tilde{f} , and continuing from (24), we have

$$\begin{aligned}
D_{[\eta_1-d+1, \eta_1+d]} &\geq \min_{\tilde{f}_{(\eta_1-d+1):(\eta_1+d)}} \max_{s_1 \in \{\eta_1-d+1, \dots, \eta_1+d+1-\tau\}} \left| \tau^{-1/2} \sum_{t=s_1}^{s_1+\tau-1} Y_t - \tilde{f}_{(\eta_1-d+1):(\eta_1+d)} \right| \\
&\geq \min_{\tilde{f}_{(\eta_1-d+1):(\eta_1+d)}} \max_{s_1 \in \{\eta_1-d+1, \dots, \eta_1+d+1-\tau\}} \left| \tau^{-1/2} \sum_{t=s_1}^{s_1+\tau-1} f_t - \tilde{f}_{(\eta_1-d+1):(\eta_1+d)} \right| \\
&- \|Z\|_{\mathcal{I}^a}.
\end{aligned} \tag{25}$$

Observe now that since f_t is symmetric around η_1 , the minimising \tilde{f} must be constant. So restrict the class of candidate fits \tilde{f} to constant. Denote the slope of f_t before the change-point by ξ . We have

$$\begin{aligned}
&\min_{\tilde{f}_{(\eta_1-d+1):(\eta_1+d)}} \max_{s_1 \in \{\eta_1-d+1, \dots, \eta_1+d+1-\tau\}} \left| \tau^{-1/2} \sum_{t=s_1}^{s_1+\tau-1} f_t - \tilde{f}_{(\eta_1-d+1):(\eta_1+d)} \right| = \\
&\frac{\tau^{1/2}}{2} \left(\frac{1}{\tau} \max_{s_1 \in \{\eta_1-d+1, \dots, \eta_1+d+1-\tau\}} \sum_{t=s_1}^{s_1+\tau-1} f_t - \frac{1}{\tau} \min_{s_1 \in \{\eta_1-d+1, \dots, \eta_1+d+1-\tau\}} \sum_{t=s_1}^{s_1+\tau-1} f_t \right) = \\
&\frac{\tau^{1/2}}{2} \xi(d-\tau).
\end{aligned} \tag{26}$$

Take $\tau = Cd$ for $C \in (0, 1)$. (25) and (26) together imply $D_{[\eta_1-d+1, \eta_1+d]} \geq C_1 \xi d^{3/2} - \|Z\|_{\mathcal{I}^a}$ for a certain universal constant C_1 . Therefore, on $\|Z\|_{\mathcal{I}^a} \leq \lambda_\alpha$, detection on $[\eta_1-d+1, \eta_1+d]$ will be triggered if $C_1 \xi d^{3/2} > 2\lambda_\alpha$, or in other words if $d \geq C_2 \lambda_\alpha^{2/3} \xi^{-2/3}$, for a large enough constant C_2 . This shows that the NSP interval of significance will be of length $O(\lambda_\alpha^{2/3} \xi^{-2/3})$.

We now discuss the slope ξ . Suppose before the symmetrisation the slopes around η_1 were ξ_1 and ξ_2 . After the symmetrisation, they are now $\xi_1 + \xi_3$ and $\xi_2 + \xi_3$ where $\xi_1 + \xi_3 = -(\xi_2 + \xi_3)$, which means $\xi = |\xi_1 - \xi_2|/2$ (w.l.o.g., $\xi > 0$). Typically, if $f_t = f(t/T)$ for a certain piecewise-linear function $f(u) : (0, 1] \rightarrow \mathbb{R}$, then $\xi = O(T^{-1})$. In the Gaussian case, we have $\lambda_\alpha = O(\sqrt{\log T})$. Therefore, if $\xi = O(T^{-1})$, then the NSP interval of significance will have the length $O(T^{2/3} \log^{1/3} T)$.

In the multiple change-point case, the argument about the relevance of Assumption 4.1 from the proof of Theorem 4.1 still applies here, and this completes the proof of the theorem. \square

Proof of Corollary 4.2. The argument is identical to the proof of Corollary 4.1. \square

I Further extensions and generalisations of NSP

I.1 NSP with autocorrelated innovations

Scenario 4 permits the use of NSP in settings in which autocorrelation is present, but this is done through the use of the lagged response as an additional covariate, rather than through allowing the innovations Z_t to be autocorrelated. We now briefly explore the case in which the Z_t 's themselves are serially correlated.

Suppose that Z_t can be modelled as an autoregressive process as follows.

$$U_t = Z_t - a_1 Z_{t-1} - \dots - a_r Z_{t-r} =: a(L)Z_t,$$

where U_t is independent (not necessarily identically distributed) noise distribution acceptable to NSP in Scenarios 1, 2 or 3, and L is the lag operator. We propose the following iterative scheme which builds on the NSP procedure for independent innovations. We use the (most general) language of Scenario 3.

Clearly, if the user knew r and (a_1, \dots, a_r) , they would be able to transform the regression problem (2) into

$$\begin{aligned} a(L)Y_t &= a(L)X_{t,\cdot}\beta^{(j)} + U_t \quad \text{for } t = \eta_j + 1 + r, \dots, \eta_{j+1}, \\ a(L)Y_t &= a(L)X_{t,\cdot}\beta^{(j,t)} + U_t \quad \text{for } t = \eta_j + 1, \dots, \eta_j + r. \end{aligned} \tag{27}$$

Due to the smoothing action of the filter $a(L)$, this now only approximates a piecewise-constant parameter regression setting, as it features the short “smooth transition” sections indexed $t = \eta_j + 1, \dots, \eta_j + r$. However, the presence of these smooth transitions does not spoil the applicability of NSP, with the intervals of significance obtained on the regression problem (27) having a similar interpretation as in the case of exactly abrupt transitions.

In practice, r or (a_1, \dots, a_r) will be unknown to the analyst. We suggest the following scheme, in which these are treated as nuisance parameters and estimated from the data, as in Fang and Siegmund (2020).

1. Similarly to Fang and Siegmund (2020), estimate r and (a_1, \dots, a_r) (to obtain, respectively, \hat{r} and $\hat{a} = (\hat{a}_1, \dots, \hat{a}_{\hat{r}})$) on a stretch of the data believed to contain no change-points.
2. Transform the regression problem using the estimated operator $\hat{a}(L)$ to obtain a problem of the form (27).
3. Run NSP suitable for independent innovations on the transformed problem, to obtain a set \mathcal{S} of the NSP intervals of significance.
4. Re-estimate r and (a_1, \dots, a_r) on the longest stretch of data outside the NSP intervals of significance.
5. Go back to step 2. and iterate until no changes are seen in the NSP intervals of significance.

I.2 Tightening the bounds: adjusting for the number p of covariates

The theoretical thresholds used by NSP, at least in the Gaussian case, appear generous: we frequently obtain the empirical coverage of 100% when e.g. 90% is asked for. The question is whether valid lower threshold could be obtained, and this calls for the re-examination of Proposition 2.1. Consider the following alternative version.

Proposition I.1 *Let the interval $[s, e]$ be such that $\forall j = 1, \dots, N \quad [\eta_j, \eta_j + 1] \not\subseteq [s, e]$. We have $D_{[s,e]} = \min_{\beta} \|Z_{s:e} - X_{s:e,\cdot}\beta\|_{\mathcal{I}_{[s,e]}^d} \leq \min_{\beta} \|Z - X\beta\|_{\mathcal{I}^d}$.*

Proof. The inequality is true because for any fixed β , the norm $\|Z - X\beta\|_{\mathcal{I}^d}$ is a maximum over a larger set than the maximum in $\|Z_{s:e} - X_{s:e,\cdot}\beta\|_{\mathcal{I}_{[s,e]}^d}$. We now prove the inequality. As $[s, e]$ does not contain a change-point, there is a β^* such that $Y_{s:e} = X_{s:e,\cdot}\beta^* + Z_{s:e}$. We have

$$\begin{aligned}
D_{[s,e]} &= \min_{\beta} \|Y_{s:e} - X_{s:e,\cdot}\beta\|_{\mathcal{I}_{[s,e]}^d} = \min_{\beta} \|X_{s:e,\cdot}\beta^* + Z_{s:e} - X_{s:e,\cdot}\beta\|_{\mathcal{I}_{[s,e]}^d} \\
&= \min_{\beta} \|Z_{s:e} - X_{s:e,\cdot}(\beta - \beta^*)\|_{\mathcal{I}_{[s,e]}^d} = \min_{\beta - \beta^*} \|Z_{s:e} - X_{s:e,\cdot}(\beta - \beta^*)\|_{\mathcal{I}_{[s,e]}^d} \\
&= \min_{\beta} \|Z_{s:e} - X_{s:e,\cdot}\beta\|_{\mathcal{I}_{[s,e]}^d}.
\end{aligned}$$

□

This leads to a tighter version of Theorem 2.1.

Theorem I.1 *Let $\mathcal{S} = \{S_1, \dots, S_R\}$ be a set of intervals returned by the NSP algorithm. The following guarantee holds.*

$$P(\exists i = 1, \dots, R \ \forall j = 1, \dots, N \ [\eta_j, \eta_j + 1] \not\subseteq S_i) \leq P(\min_{\beta} \|Z - X\beta\|_{\mathcal{I}^d} > \lambda_{\alpha}).$$

Proof. On the set $\min_{\beta} \|Z - X\beta\|_{\mathcal{I}^d} \leq \lambda_{\alpha}$, each interval S_i must contain a change-point as if it did not, then by Proposition I.1, we would have to have

$$D_{S_i} \leq \min_{\beta} \|Z - X\beta\|_{\mathcal{I}^d} \leq \lambda_{\alpha}. \quad (28)$$

However, the fact that S_i was returned by NSP means, by line 14 of the NSP algorithm, that $D_{S_i} > \lambda_{\alpha}$, which contradicts (28). This completes the proof. □

The differences with Theorem 2.1 are as follows. In Theorem 2.1, the probability $P(\exists i = 1, \dots, R \ \forall j = 1, \dots, N \ [\eta_j, \eta_j + 1] \not\subseteq S_i)$ is bounded from above by $P(\|Z\|_{\mathcal{I}^d} > \lambda_{\alpha})$, which is in turn bounded from above by $P(\|Z\|_{\mathcal{I}^a} > \lambda_{\alpha})$. These bounds are independent of the covariates X (i.e. independent of the scenario). In the Gaussian case, to choose λ_{α} , we approximated the probability $P(\|Z\|_{\mathcal{I}^a} > \lambda_{\alpha})$ using Theorem 1.3 in Kabluchko (2007) (Theorem 2.2).

By contrast, in Theorem I.1, the probability $P(\exists i = 1, \dots, R \ \forall j = 1, \dots, N \ [\eta_j, \eta_j + 1] \not\subseteq S_i)$ is bounded from above by $P(\min_{\beta} \|Z - X\beta\|_{\mathcal{I}^d} > \lambda_{\alpha})$. As $\min_{\beta} \|Z - X\beta\|_{\mathcal{I}^d} \leq \|Z - X0\|_{\mathcal{I}^d} = \|Z\|_{\mathcal{I}^d} \leq \|Z\|_{\mathcal{I}^a}$, the threshold λ_{α} obtained by solving

$$P(\min_{\beta} \|Z - X\beta\|_{\mathcal{I}^d} > \lambda_{\alpha}) = \alpha \quad (29)$$

will be lower than that obtained by solving

$$P(\|Z\|_{\mathcal{I}^d} > \lambda_{\alpha}) = \alpha \quad (30)$$

(which was done in Theorem 2.1). In addition, unlike the solution to (30), the solution to (29) accounts for the number and form of the covariates X . To solve (29), the distribution of $\min_{\beta} \|Z - X\beta\|_{\mathcal{I}^d}$ can be obtained by simulation, separately for each set of covariates X and sample size T .

We now illustrate the better localisation properties of the thus-obtained tighter bounds with a numerical example. We return to the example of Section 5.1.1, involving the piecewise-constant `blocks` signal. We simulate 100 sample paths, with the same parameters as in that section. On each sample path, we execute NSP with $\alpha = 0.1$, $M = 1000$, deterministic grid and no overlap, in two versions: (a) with the theoretical threshold as stipulated by Theorems 2.1 and 2.2, and (b) with the simulation-based threshold as in Theorem I.1 and the subsequent discussion. Both result in 100% empirical coverage. On average, NSP(a) returns 7.25 intervals, while for NSP(b) the analogous figure is 8.24 (that is, NSP(b) detects, on average, almost one change-point more than NSP(a)). Out of the 100 sample paths, NSP(a) returns more intervals in 1 case (despite the higher thresholds, this can happen due to the greedy nature of NSP), and NSP(b) in 71 cases. In the remaining 28 sample paths, the average length of an interval of significance is 80.61 for NSP(a) and 61.72 for NSP(b), a significant shortening which clearly implies better change-point localisation for NSP(b). This example illustrates the benefits of the simulation-based threshold over the theoretical threshold even for $p = 1$ covariate; the difference can only be more prominent if $p > 1$.

J Additional arguments regarding the real-data analysis

In this section, we show that the application of NSP to the real-data examples of Section 6 is justified as the errors do not exhibit significant serial correlation in the interest rate case or conditional heteroskedasticity in the price series case. Figure 8 demonstrates this for the interest rate data (note NSP was used on the scaled data shown in Figure 8, where the scaling had been performed to remove heteroscedasticity). Figure 9 shows this for the Newham house price data example (the presence of significant autocorrelation in the squared empirical residuals could have been indicative of heteroscedasticity).

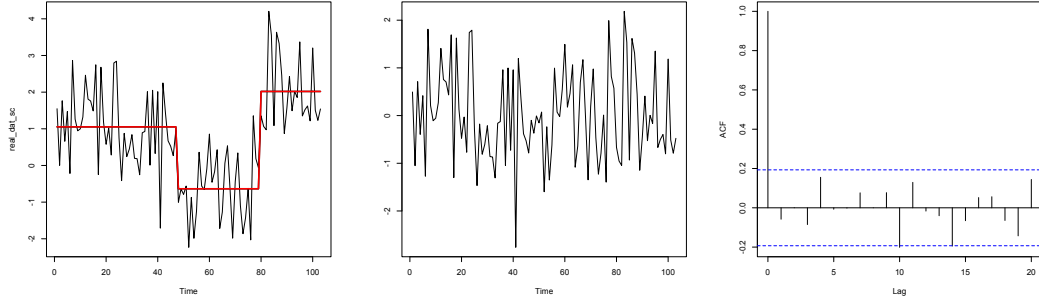


Figure 8: Left: scaled interest rate data (black) with a change-point fit obtained in R package **breakfast** (red); middle: residuals from the fit; right: their sample acf.

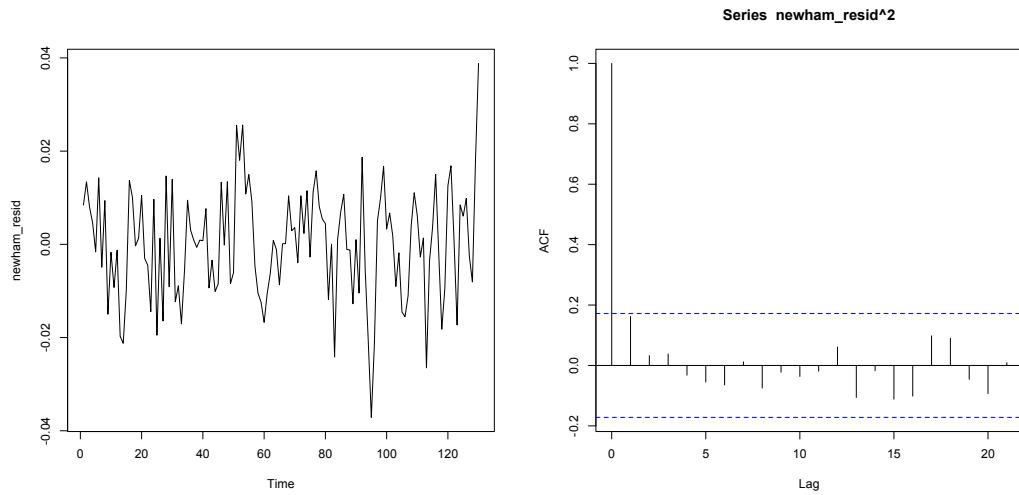


Figure 9: Left: concatenated residuals from two linear regression fits, before and after the change-point (time $t = 60$, as in the paper), in the Newham house price data; right: the sample acf of their squares.

K Discussion

We conclude with a brief discussion of a few speculative aspects of NSP.

Possible use of NSP in online monitoring for changes NSP can in principle be used in the online setting, in which ‘alarm’ should be raised as soon as Y starts deviating from linearity with respect to X . In particular, consider the following simple construction: having observed (Y_t, X_t) , $t = 1, \dots, T$, successively run NSP on the intervals $[T-1, T]$, $[T-2, T]$, \dots , until either the first interval of significance is discovered, or $[1, T]$ is reached. This will provide an answer to the question of whether the most recently observed data deviates from linearity and if so, over what time interval.

Using and interpreting NSP in the presence of gradual change If NSP is used in the absence of change-points but in the presence of gradual change, obtaining a significant interval means that it must (at global significance level α) contain some of the period of gradual change. However, this does not necessarily mean that the entire period of gradual change is contained within the given interval of significance. Note that this is the situation portrayed in Section 5.2, in which the simulation model used is a ‘gradual change’ model from the point of view of the NSP₀ method, but an ‘abrupt change’ model from the point of view of NSP₁ and NSP₂.

Possible use of NSP in testing for time series stationarity It is tempting to ask whether NSP can serve as a tool in the problem of testing for second-order stationarity of a time series. In this problem, the response Y_t would be the time series in question, while the covariates X_t would be the Fourier basis. The performance of NSP in this setting will be reported in future work.

Does the principle of NSP extend to other settings? NSP is an instance of a statistical procedure which produces intervals of significance (rather than point estimators) as an output. It is an interesting open question to what extent this emphasis on “intervals

of significance before point estimators” may extend to other settings, e.g. the problem of parameter inference in high-dimensional regression.

References

- A. Anastasiou and P. Fryzlewicz. Detecting multiple generalized change-points by isolating single ones. *Metrika*, 85:141–174, 2022.
- E. Arias-Castro, D. Donoho, and X. Huo. Near-optimal detection of geometric objects by fast multiscale methods. *IEEE Trans. Inf. Th.*, 51:2402–2425, 2005.
- J. Bai and P. Perron. Estimating and testing linear models with multiple structural changes. *Econometrica*, 66:47–78, 1998.
- J. Bai and P. Perron. Computation and analysis of multiple structural change models. *Journal of Applied Econometrics*, 18:1–22, 2003.
- R. Baranowski, Y. Chen, and P. Fryzlewicz. Narrowest-Over-Threshold detection of multiple change-points and change-point-like features. *J. Roy. Stat. Soc. Ser. B*, 81:649–672, 2019.
- H. P. Chan and G. Walther. Detection with the scan and the average likelihood ratio. *Statistica Sinica*, 23:409–428, 2013.
- Y. Chen, R. Shah, and R. Samworth. Discussion of ‘Multiscale change point inference’ by Frick, Munk and Sieling. *Journal of the Royal Statistical Society: Series B*, 76:544–546, 2014.
- D. Cheng, Z. He, and A. Schwartzman. Multiple testing of local extrema for detection of change points. *Electron. J. Statist.*, 14:3705–3729, 2020.
- P. L. Davies and A. Kovac. Local extremes, runs, strings and multiresolution. *Ann. Statist.*, 29:1–48, 2001.
- P. L. Davies, A. Kovac, and M. Meise. Nonparametric regression, confidence regions and regularization. *Ann. Stat.*, 37:2597–2625, 2009.
- H. Dette, T. Eckle, and M. Vetter. Multiscale change point detection for dependent data. *Scand. J. Statist.*, 47:1243–1274, 2020.
- L. Dümbgen and V. Spokoiny. Multiscale testing of qualitative hypotheses. *Ann. Statist.*, 29:124–152, 2001.
- L. Dümbgen and G. Walther. Multiscale inference about a density. *Ann. Stat.*, 36:1758–1785, 2008.
- V.N.L. Duy, H. Toda, R. Sugiyama, and I. Takeuchi. Computing valid p -value for optimal changepoint by selective inference using dynaming programming. In *Advances in Neural Information Processing Systems*, volume 33, pages 11356–11367, 2020.

- V. Egorov. On the asymptotic behavior of self-normalized sums of random variables. *Theory Probab. Appl.*, 41:542–548, 1997.
- B. Eichinger and C. Kirch. A MOSUM procedure for the estimation of multiple random change points. *Bernoulli*, 24:526–564, 2018.
- X. Fang and D. Siegmund. Detection and estimation of local signals. *Preprint*, 2020.
- X. Fang, J. Li, and D. Siegmund. Segmentation and estimation of change-point models: false positive control and confidence regions. *Ann. Stat.*, 48:1615–1647, 2020.
- P. Fearnhead. Exact and efficient Bayesian inference for multiple changepoint problems. *Statistics and Computing*, 16:203–213, 2006.
- K. Frick, A. Munk, and H. Sieling. Multiscale change-point inference (with discussion). *Journal of the Royal Statistical Society Series B*, 76:495–580, 2014.
- P. Fryzlewicz. Wild Binary Segmentation for multiple change-point detection. *Ann. Stat.*, 42:2243–2281, 2014.
- P. Fryzlewicz. Detecting possibly frequent change-points: Wild Binary Segmentation 2 and steepest-drop model selection. *Journal of the Korean Statistical Society*, 49:1027–1070, 2020.
- R. Garcia and P. Perron. An analysis of the real interest rate under regime shifts. *Review of Economics and Statistics*, 78:111–125, 1996.
- N. Hao, Y. Niu, and H. Zhang. Multiple change-point detection via a screening and ranking algorithm. *Statistica Sinica*, 23:1553–1572, 2013.
- S. Hyun, M. G’Sell, and R. Tibshirani. Exact post-selection inference for the generalized lasso path. *Electronic Journal of Statistics*, 12:1053–1097, 2018.
- S. Hyun, K. Lin, M. G’Sell, and R. Tibshirani. Post-selection inference for changepoint detection algorithms with application to copy number variation data. *Biometrics*, 77:1037–1049, 2021.
- X. Jeng, T. Cai, and H. Li. Optimal sparse segment identification with application in copy number variation analysis. *J. Am. Stat. Assoc.*, 105:1156–1166, 2010.
- S. Jewell, P. Fearnhead, and D. Witten. Testing for a change in mean after changepoint detection. *Journal of the Royal Statistical Society Series B*, to appear, 2022.
- Z. Kabluchko. Extreme-value analysis of standardized Gaussian increments. *Unpublished*, 2007.
- Z. Kabluchko and Y. Wang. Limiting distribution for the maximal standardized increment of a random walk. *Stoch. Proc. Appl.*, 124:2824–2867, 2014.

- C. König, A. Munk, and F. Werner. Multidimensional multiscale scanning in exponential families: limit theory and statistical consequences. *Ann. Stat.*, 48:655–678, 2020.
- S. Kovács, H. Li, P. Bühlmann, and A. Munk. Seeded binary segmentation: A general methodology for fast and optimal change point detection. *Biometrika*, to appear, 2022.
- H. Li. *Variational Estimators in Statistical Multiscale Analysis*. PhD thesis, Georg August University of Göttingen, 2016.
- H. Li and A. Munk. FDR-control in multiscale change-point segmentation. *Electronic Journal of Statistics*, 10:918–959, 2016.
- R. Meijer, T. Krebs, and J. Goeman. A region-based multiple testing method for hypotheses ordered in space or time. *Stat. Appl. Genet. Mol. Biol.*, 14:1–19, 2015.
- N. Meinshausen. Group bound: confidence intervals for groups of variables in sparse high dimensional regression without assumptions on the design. *Journal of the Royal Statistical Society Series B*, 77: 923–945, 2015.
- A. Munk, K. Proksch, H. Li, and F. Werner. Photonic imaging with statistical guarantees: From multiscale testing to multiscale estimation. In T. Salditt, A. Egner, and D. Luke, editors, *Nanoscale Photonic Imaging*, volume 134 of *Topics in Applied Physics*. Springer, 2020.
- C. F. Nam, J. Aston, and A. Johansen. Quantifying the uncertainty in change points. *J. Tim. Ser. Anal.*, 33:807–823, 2012.
- A. Nemirovski. Nonparametric estimation of smooth regression functions. *J. Comput. System Sci.*, 23:1–11, 1986.
- F. Pein, H. Sieling, and A. Munk. Heterogeneous change point inference. *J. Royal Stat. Soc. B*, 79:1207–1227, 2017.
- A. Račkauskas and C. Suquet. Invariance principles for adaptive self-normalized partial sums processes. *Stochastic Processes and Their Applications*, 95:63–81, 2001.
- A. Račkauskas and C. Suquet. Invariance principle under self-normalization for nonidentically distributed random variables. *Acta Applicandae Mathematicae*, 79:83–103, 2003.
- A. Račkauskas and C. Suquet. Hölder norm statistics for epidemic change. *Stat. Plan. Inf*, 126:495–520, 2004.
- M. Raimondo. Minimax estimation of sharp change points. *Annals of Statistics*, 26:1379–1397, 1998.
- J. Rice. Bandwidth choice for nonparametric regression. *Ann. Statist.*, 12:1215–1230, 1984.

- J. Ruanaidh and W. Fitzgerald. *Numerical Bayesian Methods Applied to Signal Processing*. Springer, 1996.
- J. Sharpnack and E. Arias-Castro. Exact asymptotics for the scan statistic and fast alternatives. *Electronic Journal of Statistics*, 10:2641–2684, 2016.
- D. Siegmund and E. S. Venkatraman. Using the generalized likelihood ratio statistic for sequential detection of a change-point. *Ann. Stat.*, 23:255–271, 1995.
- G. Walther. Optimal and fast detection of spatial clusters with scan statistics. *Ann. Stat.*, 38:1010–1033, 2010.
- D. Wang, K. Lin, and R. Willett. Statistically and computationally efficient change point localization in regression settings. *Journal of Machine Learning Research*, 22:1–46, 2021.
- Y.-C. Yao. Estimating the number of change-points via Schwarz’ criterion. *Stat. Prob. Lett.*, 6:181–189, 1988.